

osteoblasts), respectively. (F,G,L,M) Bone formation rate (BFR) in the lumbar regions (F,G) and the lateral calvarial bone (L,M) of *Id4^{+/+}* (F,L) and *Id4^{-/-}* (G,M) mice. The BFR was measured using fluorescence microscopy following double-staining with tetracycline hydrochloride (blue arrowhead) and calcein (green arrowhead). Yellow arrowheads indicate adipocytes. (J,K) Villanueva staining of the lateral calvarial bone of *Id4^{+/+}* (J) and *Id4^{-/-}* mice (K). Black arrowheads indicate osteoblasts. The original magnifications and scale bars of the images are $\times 400$ and $50\ \mu\text{m}$ (D–G), $\times 400$ and $30\ \mu\text{m}$ (H,I) and $\times 200$ and $50\ \mu\text{m}$ (J–M). (N) Bone volume (BV) to total volume (TV) ratio in the 6th lumbar bone. (O,P) BFR to bone surface (BS) ratio (O) and mineral apposition rate (MAR) (P) in the 6th lumbar bone and lateral calvarial bone. (Q,R) Number of type II osteoblasts (Q) and type IV osteoblasts (R) on the corresponding area of the lumbar BS. (S) Osteoid thickness (O. Th) in the lateral calvarial bone. N–S: *Id4^{+/+}* (n = 6), *Id4^{-/-}* (n = 6). All data were subjected to Student's t-tests. Each error bar represents the mean \pm SE. * $p < 0.05$ versus control, ** $p < 0.01$ versus control and *** $p < 0.005$ versus control. doi:10.1371/journal.pgen.1001019.g005

switch function that promotes lineage-specific differentiation (e.g. osteoblast differentiation) and inhibits alternative differentiation pathways (e.g. adipocyte differentiation). To substantiate the hypothesis, we clustered gene expression profiles during osteoblast/adipocyte differentiation and identified *Id4* as a candidate regulator of cell lineage choice. *Id* family members *Id1–4* also belong to the bHLH superfamily, but lack the DNA binding domain. Heterodimerization of *Id* proteins with other bHLH proteins facilitates dominant negative regulation. A study by Bedford *et al.* using *Id4^{-/-}* mice established *Id4* as a regulator of proliferation and differentiation of neural precursor cells [17]. Until now, however, bone and skeletal abnormalities of this mouse model have not been reported. Besides our report, expression profile studies of BMP-independent osteoblast differentiation of human MSCs and BMP2-induced osteoblast differentiation using calvarial cells derived from *Runx2*-deficient mice [25,26] demonstrated that the expression level of *Id4* gene increases during osteoblast differentiation. These results suggest that *Id4* plays an important role during osteoblast differentiation. Yet, the precise mechanism of *Id4* action and regulation remained enigmatic. We have clearly demonstrated by *in vitro* and *in vivo* loss-of-function analysis that *Id4* enhances osteogenic differentiation. Furthermore, we established a model of *Id4* playing the role of molecular switch in osteoblast differentiation of MSCs (Figure 7D). *Id4* expression increases upon BMP-induced osteoblast differentiation. Accumulating *Id4* proteins transiently interact with *Hes1*-bound *Hey2*, thus triggering the release of *Hes1* and the formation of *Id4*-*Hey2* heterodimers and *Hes1*-*Runx2* complexes. The binding of *Hes1* to *Runx2* potentiates the transcriptional activity of *Runx2* and therefore osteoblast differentiation.

Hes1 and *Hey2* are the target molecules of Notch signaling [19]. Until now, the relationship between Notch and BMP signaling pathways has been characterized by conflicting reports. On one hand experiments using ST2 cells showed that Notch1 suppresses the BMP-induced differentiation into osteoblasts [27]. On the other hand, Nobta *et al.* [28] reported that Notch signaling enhances BMP-induced osteoblast differentiation of C2C12 or MC3T3-E1 cells. At this point, there are insufficient data to resolve the controversy about the role of Notch signaling in BMP-induced osteoblast differentiation. However, our model (Figure 7D) may help to clarify the function of Notch signaling. In the absence of *Id4*, *Hes1*-*Hey2* heterodimer just occupies the promoter region of the *Runx2* target gene, whereas in the presence of *Id4*, *Id4*-*Hey2* and *Hes1*-*Runx2* complexes increase simultaneously. The concomitant increase of both complexes enhances the transcriptional activity of *Runx2*. Thus, we propose that availability and concentration of *Id4* might account for the disparate roles of Notch signaling.

In *Id4^{-/-}* mice, the drop of calvarial BFR is consistent with the phenotype of *Id1/Id3* heterozygous knockout mice. After BMP stimulation, *Id1/Id3* heterozygous knockout mice-derived calvarial cells showed reduced proliferation activity compared to calvarial cells derived from wild-type mice [29]. Thus, the decreased rate of calvarial bone formation in *Id4^{-/-}* mice might be the consequence of reduced osteoblast proliferation. The expression levels of *Id1* and *Id2* were also up-regulated in the early stage of BMP4-induced osteoblast differentiation (Figure 2A). Indeed, it has been

reported that *Id1* is an important early gene in osteoblasts after BMP stimulation [30,31]. Although the biological significance of *Id1* in the regulation of MSCs has to be elucidated in future studies, in ST2 cells, expression levels of *Id1* and *Id2* immediately returned to base levels (Figure 2C). In contrast, *Id4* expression levels in ST2 and 3T3-E1 cells continued to rise until 4 days (Figure 2C and Figure S2A) and 7 days, respectively [32].

Systemic hormones and local cytokines are known to be central regulators of bone formation. Serum levels of growth hormone (IGF1) and thyroid hormones (T3 and T4) did not change significantly between *Id4^{+/+}* and *Id4^{-/-}* mice (data not shown). Hence, impaired bone formation is most likely independent of hormonal factors and caused by repression of osteoblast differentiation.

Since the expression level of *Id4* decreases during adipocyte differentiation (Figure 2C and Figure S2B), *Id4* was believed to inhibit MSCs differentiation into adipocytes. We demonstrated that *Id4* suppression promoted adipocyte differentiation (Figure 4B–4E and Figure 8A–8E), but *Id4* overexpression slightly decreased lipid accumulation level in ST2 adipocytes (Figure 4G). In an effort to shed light on the molecular mechanism, we assayed the expression level of *Ppar γ 2*, a master regulator of adipocyte differentiation. *Ppar γ 2* expression increased in adipogenic-induced ST2 cells when *Id4* was knocked down (Figure 4B) and in bone marrow cells of femur and tibia of *Id4^{-/-}* mice (Figure 8F). However, the results of luciferase reporter assays ruled out effects of *Id4* on the promoter activity of *Ppar γ 2* (data not shown). *Ppar γ 2* down-regulation by *Id4* might involve a yet unknown, indirect regulatory mechanism. We noticed that the number of osteoclasts increased in the tibial epiphyseal regions and the 6th lumbar vertebra (data not shown). In view of an earlier report on *Ppar γ* promoting osteoclast differentiation by activating *c-fos* [33], we interpret the increased number of adipocytes and osteoclasts in 6th lumbar and tibial bone of *Id4^{-/-}* mice as a result of indirect activation of *Ppar γ 1* and/or *Ppar γ 2* transcriptional activity by lack of *Id4*. To corroborate these assumptions, additional analyses of the relationships and interactions of *Id4*, *Ppar γ* and *c-fos* in context of adipocyte and osteoclast differentiation are necessary.

In summary, delineating clusters of transcription factors is a powerful strategy to identify cell fate-determining members of regulatory networks. Concerted application of our genome-wide expression profiling analyses and validation of transcription factor candidate regulators synthesize knowledge of specific molecular mechanism underlying osteoporosis and/or metabolic disease. In case of *Id4*, our findings reflect the potential pen-ultimate position of *Id4* in the *Runx2* activation/repression, which permits the differential integration of various upstream signals. Since BMP and Notch signaling affect osteoblast differentiation at different phases of differentiation, modulation of *Id4* expression may create new venues for treating the onset of osteoporosis.

Materials and Methods

Cell culture

ST2 cells were obtained from RIKEN BioResource Center (BRC, Tsukuba, Japan) and cultured as described [34]. Primary

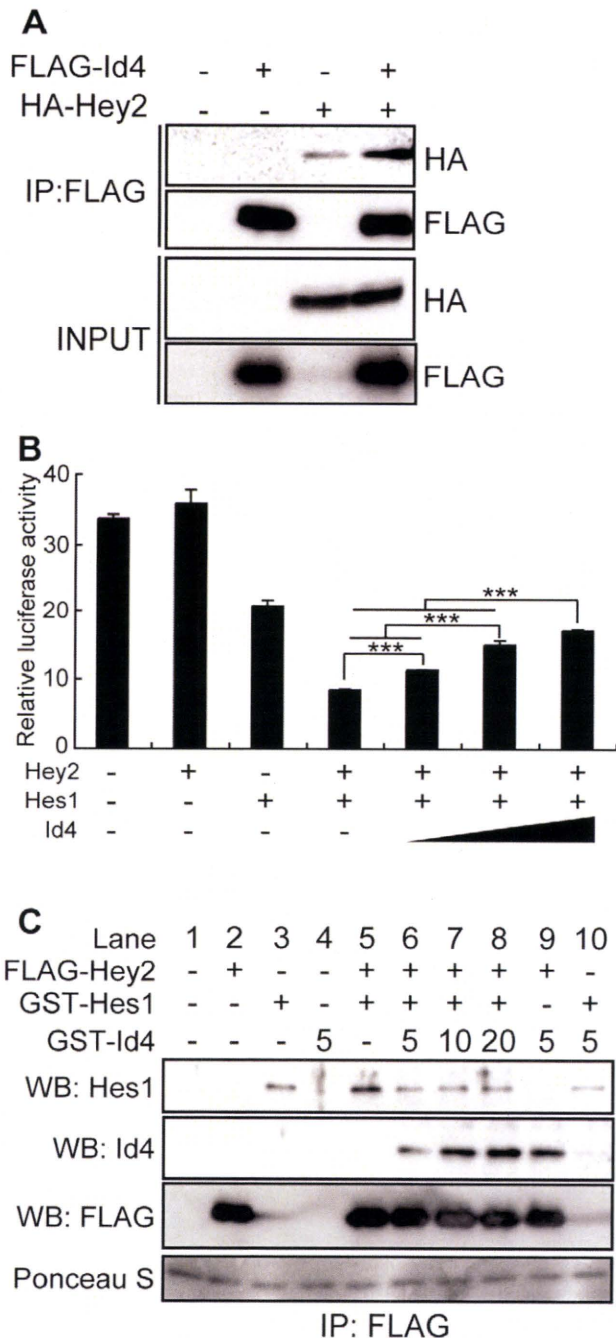


Figure 6. Id4 interacts with Hey2 and inhibits the suppression of reporter activity by Hey2/Hes1 complex. (A) Interaction of FLAG-tagged Id4 (FLAG-Id4) and human influenza hemagglutinin-tagged Hey2 (HA-Hey2) was confirmed in 293FT cells by immunoprecipitation (IP). (B) CV1 cells transfected with 6×E-box luciferase reporter, Hey2 and Hes1 expression vectors and with increasing doses of Id4 expression vector. Luciferase assay data were subjected to Student's *t*-tests. Each error bar represents the mean \pm SE of triplicates. ****p*<0.005 versus control. (C) *In vitro* assay of Id4 dose-dependent attenuation of Hey2-Hes1 complex interaction. GST-Id4 volume added was 5, 10 and 20 μ l, respectively. WB: Western blotting. doi:10.1371/journal.pgen.1001019.g006

osteoblasts were isolated from *Id4*^{+/+} and *Id4*^{-/-} neonatal calvarial bone as described previously [35]. Osteogenic differentiation was induced by changing the medium every three days to culture medium supplemented with 100 ng/ml of bone morpho-

genetic protein 4 (BMP4) (R&D Systems, Minneapolis, MN) and adipogenic differentiation was induced by changing the medium to differentiation medium supplemented with 10% fetal bovine serum (FBS), 0.5 mM 3-isobutyl-1-methylxanthine, 0.25 μ M dexamethasone, and insulin-transferrin-selenium-X supplement containing 5 μ g/ml of insulin (Invitrogen, Carlsbad, CA) and 1 μ M rosiglitazone. After 48 hr, the differentiation medium was replaced with culture medium supplemented with 10% FBS.

Id4 knockdown by siRNA

siRNA sequences targeting the mouse *Id4* transcript were purchased from Ambion (for adipocyte) and Invitrogen (for osteoblast). AllStar Negative Control siRNA (QIAGEN, cat. No., 1027281) and Negative Universal Control Med#2 (Invitrogen, cat. No., 12935-112) was used as a negative control in adipocyte and osteoblast differentiation, respectively. The sequences of siRNA used for *Id4* knockdown were as follows; sense, CCUUUGUAUUUGACGUGUAtt; antisense, UACACGUCAAAACAAAGGtt (Ambion, cat No. AM16704, ID. 159536); for adipocyte differentiation; sense, UUAUUUCUGCUCUGGCCUCCUU; antisense, AAGGAGGGCCAGAGCAGAAAUAUAA (Invitrogen, stealth_455, cat No. 10620312); for osteoblast differentiation. For siRNA transfection, a complex of Lipofectamine 2000 (Invitrogen) and 20 nM siRNA was prepared according to the manufacturer's instruction and directly mixed with cells in the culture plates. The medium was replaced at 4–6 hr after transfection with fresh differentiation medium (adipogenic induction) or 10% FBS supplemented with 100 ng/ml of BMP4 (osteogenic induction).

Lipid assay and Alkaline phosphatase (ALP) staining

Lipid accumulation in adipocytes was detected by using Oil Red O staining as described previously [36]. The triglyceride content in adipocytes was determined as follows. ST2 cells were washed with cold phosphate-buffered saline (PBS) and total lipids were extracted with chloroform/methanol (2:1, v/v). The lower organic phase was dried, and the lipids were dissolved in 2-propanol. The triglyceride content was measured using Triglyceride E-test (Wako, Japan) according to the manufacturer's instructions. Protein concentrations were determined with Quick Start Bradford Dye Reagent (BIO RAD, 500-0205), using bovine gamma globulin as standard. ALP staining and measurements were performed as described previously [34].

Isolation of total RNA and quantitative real-time PCR (qRT-PCR)

Total RNA was isolated from liver, brain, kidney, thymus, brown adipose tissue (BAT), heart, white adipose tissue (WAT), adrenal gland, cortical bone, calvaria, bone marrow and posterior limb of E18.5 mouse embryo using TRIzol reagent (Invitrogen) and RNeasy columns (QIAGEN, Hilden, Germany) according to the manufacturer's instructions. Bone marrow was obtained by slicing of the ends of femur and tibia bones and then flushing it out with PBS using a syringe. Yield and quality of RNA were determined with a NanoDrop spectrometer (NanoDrop Technology, San Diego, CA) and a BioAnalyzer (Agilent Technologies, Santa Clara, CA). Gene expression levels were measured by qRT-PCR as described previously [34]. The sequences of forward and reverse primers used for each gene amplification were as follows; *gapdh*, GAPDH_768Fw_qPCR 5'-TGGAGAAACCTGCCAAGTATG-3', GAPDH_889Rv_qPCR 5'-GGAGACAACCTGGT-CCTCAG-3'; *Id4*, Mm_Id4_532Fw 5'-AGGGTGACAGCATTCTCTGC-3', Mm_Id4_658Rv 5'-CCGGTGGCTTGTTTC-TCTTA-3'; *Ppar γ 2*, PPAR γ 2Fw 5'-ATGGGTGAAACTCTGG-

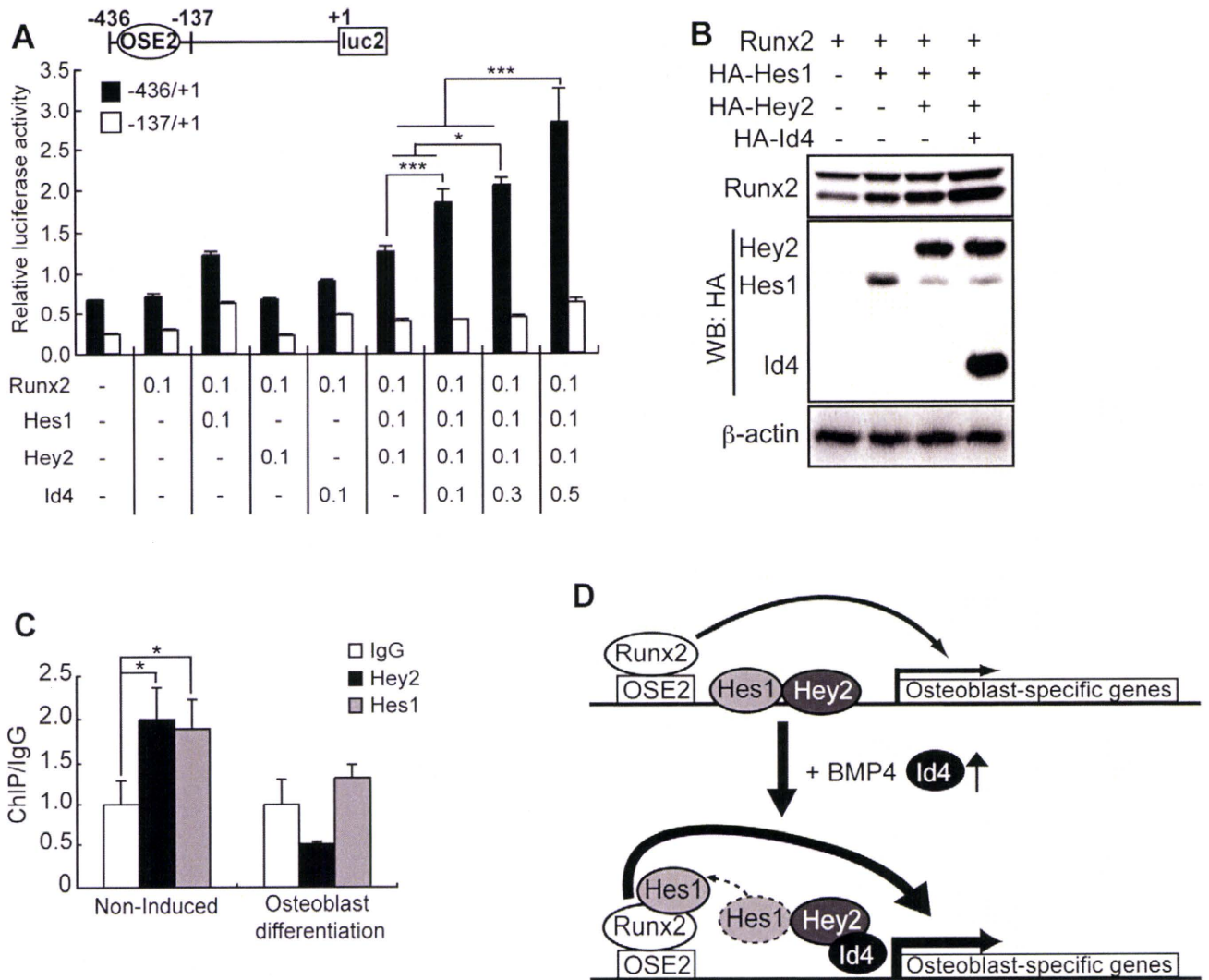


Figure 7. Id4 enhanced Runx2 transcriptional activity through stabilization of Runx2 protein. (A) Relative luciferase activity of *Bglap1* promoter in CV1 cells transfected with Runx2, Hes1, Hey2 and Id4 expression vectors. *Bglap1* promoter luciferase reporters were used as Runx2-dependent (-436bp/+1bp) or Runx2-independent (-137bp/+1bp). Luciferase assay data were subjected to Student's t-tests. Each error bar represents the mean \pm SE of triplicates. * $p < 0.05$ versus control and *** $p < 0.005$ versus control. +1; transcription start site, bp; base pair. (B) Western blot analysis of Cos7 whole cell lysate using anti-Runx2, anti-HA and anti- β -actin (loading control) antibodies. The stability of Runx2-Hes1 complex increased in the presence of Id4. (C) ChIP-qPCR analyses of Hey2 and Hes1 binding onto *Bglap1* promoter in ST2 cells at day 4 after induction of osteoblast differentiation or non-induced ST2 cells. (D) A model of Id4 promoting Runx2-induced osteoblast differentiation. doi:10.1371/journal.pgen.1001019.g007

GAGA-3', PPAR γ 2-1Rv 5'-GAGCTGATTCCGAAGTTGGT-3'; *Bglap1*, OC(PM15547142)Fw 5'-CTCTGTCTCTC TGAC-CTCACAG-3', OC(PM15547142)Rv 5'-GGAGCTGCTGTGACATCCATAC-3'; *Adipoq*, Mm_AdipoQ_298Fw 5'-GATGGCACTCCTGGAGAGAA-3', Mm_AdipoQ_443Rv 5'-GCTTC-TCCAGGCTCTCCTTT-3'.

Expression microarray experiments

RNA was extracted from differentiating ST2 osteoblasts and adipocytes after induction of differentiation, using PureLink miRNA Isolation Kit (Invitrogen) according to the manufacturer's instructions for total RNA purification. Total RNA derived from ST2 at 0 hr was used as control. Biotin-labeled cRNA was synthesized as recommended by Affymetrix guidelines. Labeled samples were hybridized to the Affymetrix GeneChip Mouse Genome 420 2.0 arrays according to the manufacturer's protocol.

Scanning and intensity data analysis was performed as described elsewhere [37].

Expression profiling analyses in ST2 osteoblast and adipocyte differentiation

Collected microarray expression data was background-subtracted, and normalized using the robust multi-array analysis method [37]. Differentially expressed genes were determined by selecting expression subgroups that contained the probe sets of up/down-regulated genes. Genes were considered up-regulated (down-regulated) if their log₂ intensity ratio was greater (less) than 1 (-1), or greater (less) than the mean plus (minus) 3-times standard deviation. All gene and probe set annotations were derived from Ensembl release 52. Genes with transcription-related Gene Ontology (GO) annotations (Table 3) were considered as transcription factor-coding genes. Genes with

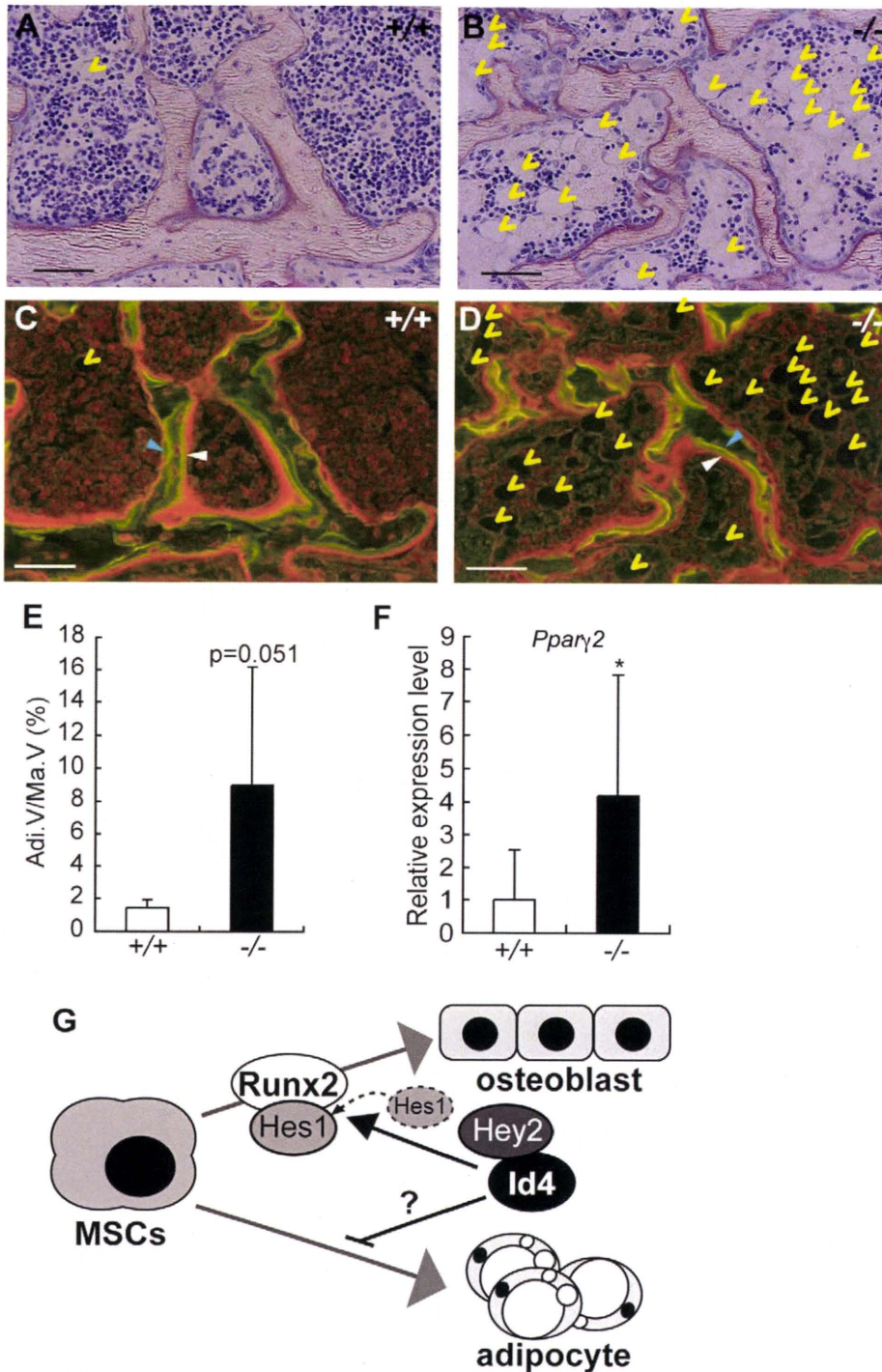


Figure 8. 4-week-old *Id4*^{-/-} mice show increased adipocytes in bone marrow. (A,B) Villanueva staining of epiphyseal tibia of *Id4*^{+/+} (A) and *Id4*^{-/-} mice (B). (C,D) The BFR was measured in the tibial epiphysial regions in *Id4*^{+/+} (C) and *Id4*^{-/-} mice (D) using a fluorescence microscopy following double-staining with tetracycline hydrochloride (blue arrowheads) and calcein (white arrowheads). Yellow arrowheads indicate adipocytes. The original magnifications and scale bars of the images are $\times 400$ and $100\ \mu\text{m}$. (E) The total area occupied by adipocytes (Adi.V) in the epiphyseal tibia bone marrow. *Id4*^{+/+} (n=6), *Id4*^{-/-} (n=6). (F) *Pparγ2* mRNA expression is significantly elevated in bone marrow cells of *Id4*^{-/-} compared to *Id4*^{+/+} mice. Relative expression levels of *Pparγ2* mRNA were measured by qRT-PCR. *Id4*^{+/+} (n=9), *Id4*^{-/-} (n=10). All data were subjected to Student's t-tests. Each error bar represents the mean \pm SE. **p* < 0.05 versus control. (G) The role of *Id4* in bone formation and bone marrow environment. doi:10.1371/journal.pgen.1001019.g008

InterPro accession IPR001092 were annotated as bHLH transcription factor-coding genes. Spotfire DecisionSite version 8.1.1 (TIBCO Software, Inc.) was used for hierarchical clustering and generating the gene expression heat maps.

Luciferase reporter assays

Bglap1 promoter regions were cloned by PCR from the mouse genome. 6 \times E-box sequence (CGCGTCCACGTGGGGCCACGTGGGGCCACGTGGGGCCACGTGGG GCCACGTGGG-

Table 3. Gene ontology IDs and terms (GO release 2009-01-25) associated with 1,270 transcription factors of Table 1.

GO ID	GO Term
GO:0000156	two-component response regulator activity
GO:0003700	transcription factor activity
GO:0003701	RNA polymerase I transcription factor activity
GO:0003702	RNA polymerase II transcription factor activity
GO:0003704	specific RNA polymerase II transcription factor activity
GO:0003705	RNA polymerase II transcription factor activity, enhancer binding
GO:0003706	ligand-regulated transcription factor activity
GO:0003709	RNA polymerase III transcription factor activity
GO:0003711	transcription elongation regulator activity
GO:0003712	transcription cofactor activity
GO:0003713	transcription coactivator activity
GO:0003714	transcription corepressor activity
GO:0003715	transcription termination factor activity
GO:0003716	RNA polymerase I transcription termination factor activity
GO:0003717	RNA polymerase II transcription termination factor activity
GO:0003718	RNA polymerase III transcription termination factor activity
GO:0008140	cAMP response element binding protein binding
GO:0008148	negative transcription elongation factor activity
GO:0008159	positive transcription elongation factor activity
GO:0016251	general RNA polymerase II transcription factor activity
GO:0016252	nonspecific RNA polymerase II transcription factor activity
GO:0016455	RNA polymerase II transcription mediator activity
GO:0016563	transcription activator activity
GO:0016564	transcription repressor activity
GO:0016565	general transcriptional repressor activity
GO:0016566	specific transcriptional repressor activity
GO:0016943	RNA polymerase I transcription elongation factor activity
GO:0016944	RNA polymerase II transcription elongation factor activity
GO:0016945	RNA polymerase III transcription elongation factor activity
GO:0016986	transcription initiation factor activity
GO:0016987	sigma factor activity
GO:0016988	transcription initiation factor antagonist activity
GO:0016989	sigma factor antagonist activity
GO:0017163	negative regulator of basal transcription activity
GO:0030374	ligand-dependent nuclear receptor transcription coactivator activity
GO:0030375	thyroid hormone receptor coactivator activity
GO:0030401	transcription antiterminator activity
GO:0030528	transcription regulator activity
GO:0042156	zinc-mediated transcriptional activator activity

doi:10.1371/journal.pgen.1001019.t003

GCCACGTGGGGA) and cloned fragments were ligated to the firefly luciferase gene (derived from pGL4.10, Promega). CV1 cells were co-transfected with the firefly luciferase reporter vectors, expression vectors and the internal control Renilla luciferase vector (pGL4.74, Promega) using Lipofectamine 2000 (Invitrogen). Luciferase activities were measured with Wallac 1420 Multilabel counter (PerkinElmer Life and Analytical Sciences, Turku, Finland). These experiments were performed in triplicate.

Co-immunoprecipitation and GST-pull down assay

Cos7 cells were transfected with FLAG-Id4 expression vector with either HA tagged expression vector (Hes1, Hey1, Hey2, Bhlhc40). The extracts from the transfected cells were incubated with Protein G sepharose beads and precipitated with either anti-FLAG antibody (SIGMA) or normal mouse IgG (Santa cruz) overnight at 4°C. After washing with PBS, bound proteins were separated by SDS-PAGE followed by Western blot analysis with anti-HA antibody, anti-FLAG antibody. GST-Id4 expression vector, Flag-Hey2 expression vector and Flag-empty vector were expressed in *E.coli*. The crude extract of GST-Id4 or GST expressed in *E.coli* was incubated with glutathione sepharose beads for 4 hr at 4°C. The precipitate was incubated with the extract of Flag-Hey2 overnight at 4°C. After washing, the bound proteins were separated by SDS-PAGE followed by Western blot analysis with anti-Flag antibody.

Chromatin Immunoprecipitation (ChIP)-qPCR analysis

ChIP was performed as described previously [38]. ST2 cells were cultured for 4 days with or without 100 ng/ml BMP4, respectively. The antibodies used for ChIP were anti-Hey2 (Protein Tech Group, cat No. 10597-1-AP), anti-Hes1 (Santa Cruz, H-140) and normal rabbit IgG (Santa Cruz, sc-2027) as negative control. Forward and reverse qPCR primer sequences contained OSE2 of the *Bglap1* promoter (Bglap2_ChIP_L789, 5'-GATTGTGGCCTCTCGTC-3'; Bglap2_ChIP_R8, 5'-ATCG-GCTACTCTGTGCTCT-3').

Animals

Id4^{-/-} mice previously generated by Bedford et al. (2005) were kindly supplied by Dr. Kondo who received them originally from Dr. Sablitzky (University of Nottingham). All mice used in this study were maintained and handled according to the protocols approved by the Animal Research Committee of Saitama Medical University.

Bone morphometric measurements

To assess the static and dynamic parameters of bone histomorphometry, 3 weeks old female mice were labeled with intraperitoneal injections of 20 mg/kg of tetracycline hydrochloride (Sigma) at 4 days before sacrifice. Two days before sacrifice, the mice were injected with 10 mg/kg of calcein (Dojindo Co., Kumamoto, Japan). Tibiae and lumbar vertebrae were removed from each mouse, and fixated with 70% ethanol. The bones were trimmed to remove the muscle, stained with Villanueva bone stain for 5 days, dehydrated in graded concentrations of ethanol, and embedded in methyl-methacrylate (Wako Chemicals, Kanagawa, Japan) without decalcification. Sagittal plane sections (5 μm thick) of the lumbar vertebrae were cut using a Microtome (Leica, Germany). Bone morphometric analyses were performed using a semi-automatic image analyzing system software (System Supply, Nagano, Japan) and Optiphot fluorescent microscope (Nikon, Tokyo, Japan).

Supporting Information

Figure S1 Heat-map of osteoblast differentiation phase-specific up-regulated transcription factor genes. Transcription factors of the bHLH family are indicated by purple bars. The column 'Cluster groups' shows the gene symbols of up-regulated transcription factors in time-sequential (chronological) cluster order. The gene symbols of the up-regulated transcription factors are listed in the same order as they appear on the image. Phase 1 (1hr; 46 transcription factors): *Foxc2*, *Nfatc1*, *Hoxb2*, *Fkhl18*,

Med14, Id4, Mx2, Id2, Ankrd1, Hes1, Bhlhe40, Foxn1, Tle4, Hmga2, Dlx3, Gata2, Dlx2, Nr4a3, Axud1, Eaf1, Hipk2, AC153948.5, Zfx, Cebpb, Grhl1, Smad7, Rel, Maff, Mafk, Klf16, Id1, Nfil3, Fosl1, Klf5, Npas4, Lmcd1, Atf3, Fosl, Mef2c, Erf, Mef2a, Atp6v0a1, Srf, Tgfb1, Nr4a1 and Junb; phase 2 (6–24hr; 29 transcription factors); Hey1, Atoh8, Helb, Hdac9, Atf6, Gcom1, Hoxa1, Prrx1, Tgfb1, Creb3l1, Rbm9, Elk3, C1d, Dlx1, Pde8a, Hey2, Ets2, Dtna, Smad6, Foxo1, Cux1, Gatad2b, Irf5, Rfc1, Sp7, Arnt2, Aebp1, Hoxc13 and Aff3; phase 3 (30–48hr; 4 transcription factors): Lef1, Fabp4, Stat5a, Prrx2; phase 4 (4–6d; 7 transcription factors): Hod, Maf, Foxf2, Sox9, Stat1, Foxd1 and Neol; phase 5 (8–14d; 24 transcription factors): Stat2, Esr1, Klf9, Klf13, AC162313.5, Cml3, Pou6f1, Pura, Nfat5, Zfp521, Trib3, Ddit3, 2210012G02Rik, Clock, Irf7, Nr3c1, Irf9, Zhx2, Sqstm1, Znf1, Atf5, Hoxa9, Nr1d2 and Nfe2l1.

Found at: doi:10.1371/journal.pgen.1001019.s001 (1.10 MB TIF)

Figure S2 *Id4* expression pattern in ST2 osteoblast (A) and adipocyte (B) differentiation. Relative expression levels of *Id4* mRNA were measured by qRT-PCR.

Found at: doi:10.1371/journal.pgen.1001019.s002 (0.16 MB TIF)

Figure S3 4-week-old *Id4*^{-/-} mice show decrease of growth plate in tibia. (A,B) Villanueva staining of growth plate of *Id4*^{+/+} (A) and *Id4*^{-/-} (B) mice tibia. The original magnifications and scale bars of the images are $\times 64$ and 500 μ m. (C) Growth plate width in tibia. (D) Longitudinal Growth Rate (Lo. G. R) in tibia. All data were subjected to Student's t-tests. $***p < 0.005$ versus control. Each error bar represents the mean \pm SE of *Id4*^{+/+} (n = 6) and *Id4*^{-/-} (n = 6), respectively.

Found at: doi:10.1371/journal.pgen.1001019.s003 (2.67 MB TIF)

Figure S4 *Id4* associates with *Hey2*. (A) Isolation of bHLH transcription factor binding with *Id4* was performed by immunoprecipitation (IP). IP was carried out using anti-FLAG antibody and Western blot analysis (WB) was performed using anti-HA antibody. Arrowheads indicate that *Hey2* binds with *Id4*. (B) Direct interaction of recombinant glutathione S-transferase-tagged *Id4* (GST-*Id4*) and recombinant FLAG-tagged *Hey2* (FLAG-*Hey2*) was confirmed *in vitro*. The GST-pull down assay performed using glutathione sepharose beads bound to recombi-

nant GST-*Id4*. Recombinant FLAG-*Hey2* was detected with anti-FLAG antibody.

Found at: doi:10.1371/journal.pgen.1001019.s004 (0.22 MB TIF)

Figure S5 Expression level of osteoblast marker *in vivo*. (A) Ratio of relative *Bglap1* mRNA expression level between osteoblast-induced POB and non-induced POB from *Id4*^{+/+} and *Id4*^{-/-} neonatal calvarial bone. *Id4*^{+/+} (n = 37), *Id4*^{-/-} (n = 21). qRT-PCR data were subjected to Student's t-tests. $**p < 0.01$ versus control. (B) Relative expression levels of *Id4* and *Bglap1* mRNA in *Id4*^{+/+} and *Id4*^{-/-} mouse embryo (E18.5) posterior limb were measured by qRT-PCR. *Id4*^{+/+} (n = 1), *Id4*^{-/-} (n = 4). Each error bar represents the mean \pm SE of triplicates.

Found at: doi:10.1371/journal.pgen.1001019.s005 (0.18 MB TIF)

Table S1 List of transcription factors expressed in induced ST2 cells differentiating into osteoblasts or adipocytes. *Bhlh* members are indicated using bold type. Arrows indicate up- (\uparrow), down-regulated (\downarrow), or up- and down-regulated ($\uparrow\downarrow$) transcription factors. No change in expression levels is symbolized by the almost equal sign (\approx).

Found at: doi:10.1371/journal.pgen.1001019.s006 (0.10 MB XLS)

Acknowledgments

We greatly appreciate the technical assistance of M. Iseki, S. Okumura, M. Kitazato, M. Otsu, and K. Tanaka. We are grateful to K. Kano, M. Kohda, A. Itoh, H. Asahara, Y. Ito, and H. Iseki for their thoughtful discussion. We thank Y. Hayashizaki, J. Kawai, and H. Suzuki for critical suggestions and supporting the project.

Author Contributions

Conceived and designed the experiments: Y Tokuzawa, K Yagi, Y Mizuno, Y Okazaki. Performed the experiments: Y Tokuzawa, K Yagi, Y Yamashita, Y Ninomiya, Y Kanesaki-Yatsuka, M Akita, H Motegi, S Wakana, T Noda, Y Mizuno. Analyzed the data: Y Tokuzawa, Y Yamashita, Y Nakachi, I Nikaido, H Bono. Contributed reagents/materials/analysis tools: F Sablitzky, S Arai, R Kurokawa, T Fukuda, T Katagiri. Wrote the paper: Y Tokuzawa, K Yagi, Y Nakachi, C Schönbach, T Suda, Y Okazaki.

References

- Burkhardt R, Kettner G, Bohn W, Schmidmeier M, Schlag R, et al. (1987) Changes in trabecular bone, hematopoiesis and bone marrow vessels in aplastic anemia, primary osteoporosis, and old age: a comparative histomorphometric study. *Bone* 8: 157–164.
- Nuttall ME, Gimble JM (2004) Controlling the balance between osteoblastogenesis and adipogenesis and the consequent therapeutic implications. *Curr Opin Pharmacol* 4: 290–294.
- Akune T, Ohba S, Kamekura S, Yamaguchi M, Chung UI, et al. (2004) PPAR γ insufficiency enhances osteogenesis through osteoblast formation from bone marrow progenitors. *J Clin Invest* 113: 846–855.
- Kobayashi H, Gao Y, Ueta C, Yamaguchi A, Komori T (2000) Multilineage differentiation of *Cbfa1*-deficient calvarial cells *in vitro*. *Biochem Biophys Res Commun* 273: 630–636.
- Lian JB, Stein GS, Javed A, van Wijnen AJ, Stein JL, et al. (2006) Networks and hubs for the transcriptional control of osteoblastogenesis. *Rev Endocr Metab Disord* 7: 1–16.
- Nishimura R, Hata K, Ikeda F, Ichida F, Shimoyama A, et al. (2008) Signal transduction and transcriptional regulation during mesenchymal cell differentiation. *J Bone Miner Metab* 26: 203–212.
- Takada I, Mihara M, Suzawa M, Ohtake F, Kobayashi S, et al. (2007) A histone lysine methyltransferase activated by non-canonical Wnt signalling suppresses PPAR- γ transactivation. *Nat Cell Biol* 9: 1273–1285.
- Iwata T, Kawamoto T, Sasabe E, Miyazaki K, Fujimoto K, et al. (2006) Effects of overexpression of basic helix-loop-helix transcription factor *Decl* on osteogenic and adipogenic differentiation of mesenchymal stem cells. *Eur J Cell Biol* 85: 423–431.
- Buskin JN, Hauschka SD (1989) Identification of a myocyte nuclear factor that binds to the muscle-specific enhancer of the mouse muscle creatine kinase gene. *Mol Cell Biol* 9: 2627–2640.
- Arnold HH, Braun T (1996) Targeted inactivation of myogenic factor genes reveals their role during mouse myogenesis: a review. *Int J Dev Biol* 40: 345–353.
- Kim JB, Spiegelman BM (1996) ADD1/SREBP1 promotes adipocyte differentiation and gene expression linked to fatty acid metabolism. *Genes Dev* 10: 1096–1107.
- Ross SE, Greenberg ME, Stiles CD (2003) Basic helix-loop-helix factors in cortical development. *Neuron* 39: 13–25.
- Ross DA, Hannehalli S, Tobias JW, Cooch N, Shiekhattar R, et al. (2006) Functional analysis of *Hes-1* in preadipocytes. *Mol Endocrinol* 20: 698–705.
- Lee JS, Thomas DM, Gutierrez G, Carty SA, Yanagawa S, et al. (2006) *HES1* cooperates with pRb to activate *RUNX2*-dependent transcription. *J Bone Miner Res* 21: 921–933.
- Tontonoz P, Hu E, Graves RA, Budavari AI, Spiegelman BM (1994) mPPAR γ 2: tissue-specific regulator of an adipocyte enhancer. *Genes Dev* 8: 1224–1234.
- Hu E, Liang P, Spiegelman BM (1996) *AdipoQ* is a novel adipose-specific gene dysregulated in obesity. *J Biol Chem* 271: 10697–10703.
- Bedford L, Walker R, Kondo T, van Cruchten I, King ER, et al. (2005) *Id4* is required for the correct timing of neural differentiation. *Dev Biol* 280: 386–395.
- Sun XH, Copeland NG, Jenkins NA, Baltimore D (1991) *Id* proteins *Id1* and *Id2* selectively inhibit DNA binding by one class of helix-loop-helix proteins. *Mol Cell Biol* 11: 5603–5611.
- Iso T, Sartorelli V, Poizat C, Iezzi S, Wu HY, et al. (2001) *HERP*, a novel heterodimer partner of *HES/E(spl)* in Notch signaling. *Mol Cell Biol* 21: 6080–6089.
- Komori T, Yagi H, Nomura S, Yamaguchi A, Sasaki K, et al. (1997) Targeted disruption of *Cbfa1* results in a complete lack of bone formation owing to maturational arrest of osteoblasts. *Cell* 89: 755–764.

21. Otto F, Thornell AP, Crompton T, Denzel A, Gilmour KC, et al. (1997) *Cbfa1*, a candidate gene for cleidocranial dysplasia syndrome, is essential for osteoblast differentiation and bone development. *Cell* 89: 765–771.
22. Nakashima K, Zhou X, Kunkel G, Zhang Z, Deng JM, et al. (2002) The novel zinc finger-containing transcription factor *osterix* is required for osteoblast differentiation and bone formation. *Cell* 108: 17–29.
23. Ducy P, Karsenty G (1995) Two distinct osteoblast-specific cis-acting elements control expression of a mouse osteocalcin gene. *Mol Cell Biol* 15: 1858–1869.
24. Suh JH, Lee HW, Lee JW, Kim JB (2008) *Hes1* stimulates transcriptional activity of *Runx2* by increasing protein stabilization during osteoblast differentiation. *Biochem Biophys Res Commun* 367: 97–102.
25. Kulterer B, Friedl G, Jandrositz A, Sanchez-Cabo F, Prokesch A, et al. (2007) Gene expression profiling of human mesenchymal stem cells derived from bone marrow during expansion and osteoblast differentiation. *BMC Genomics* 8: 70.
26. Liu T, Gao Y, Sakamoto K, Minamizato T, Furukawa K, et al. (2007) BMP-2 promotes differentiation of osteoblasts and chondroblasts in *Runx2*-deficient cell lines. *J Cell Physiol* 211: 728–735.
27. Sciaudone M, Gazzero E, Priest L, Delany AM, Canalis E (2003) Notch 1 impairs osteoblastic cell differentiation. *Endocrinology* 144: 5631–5639.
28. Nobta M, Tsukazaki T, Shibata Y, Xin C, Moriishi T, et al. (2005) Critical regulation of bone morphogenetic protein-induced osteoblastic differentiation by *Delta1/Jagged1*-activated Notch1 signaling. *J Biol Chem* 280: 15842–15848.
29. Maeda Y, Tsuji K, Nifuji A, Noda M (2004) Inhibitory helix-loop-helix transcription factors *Id1/Id3* promote bone formation in vivo. *J Cell Biochem* 93: 337–344.
30. Katagiri T, Imada M, Yanai T, Suda T, Takahashi N, et al. (2002) Identification of a BMP-responsive element in *Id1*, the gene for inhibition of myogenesis. *Genes Cells* 7: 949–960.
31. Lopez-Rovira T, Chalaux E, Massague J, Rosa JL, Ventura F (2002) Direct binding of *Smad1* and *Smad4* to two distinct motifs mediates bone morphogenetic protein-specific transcriptional activation of *Id1* gene. *J Biol Chem* 277: 3176–3185.
32. Zhang Y, Hassan MQ, Li ZY, Stein JL, Lian JB, et al. (2008) Intricate gene regulatory networks of helix-loop-helix (HLH) proteins support regulation of bone-tissue related genes during osteoblast differentiation. *J Cell Biochem* 105: 487–496.
33. Wan Y, Chong LW, Evans RM (2007) PPAR-gamma regulates osteoclastogenesis in mice. *Nat Med* 13: 1496–1503.
34. Mizuno Y, Yagi K, Tokuzawa Y, Kanesaki-Yatsuka Y, Suda T, et al. (2008) miR-125b inhibits osteoblastic differentiation by down-regulation of cell proliferation. *Biochem Biophys Res Commun* 368: 267–272.
35. Yang S, Takahashi N, Yamashita T, Sato N, Takahashi M, et al. (2005) Muramyl dipeptide enhances osteoclast formation induced by lipopolysaccharide, IL-1 alpha, and TNF-alpha through nucleotide-binding oligomerization domain 2-mediated signaling in osteoblasts. *J Immunol* 175: 1956–1964.
36. Yagi K, Kondo D, Okazaki Y, Kano K (2004) A novel preadipocyte cell line established from mouse adult mature adipocytes. *Biochem Biophys Res Commun* 321: 967–974.
37. Irizarry RA, Bolstad BM, Collin F, Cope LM, Hobbs B, et al. (2003) Summaries of Affymetrix GeneChip probe level data. *Nucleic Acids Res* 31: e15.
38. Wakabayashi K, Okamura M, Tsutsumi S, Nishikawa NS, Tanaka T, et al. (2009) The peroxisome proliferator-activated receptor gamma/retinoid X receptor alpha heterodimer targets the histone modification enzyme PR-Set7/Setd8 gene and regulates adipogenesis through a positive feedback loop. *Mol Cell Biol* 29: 3544–3555.



BMP signalling permits population expansion by preventing premature myogenic differentiation in muscle satellite cells

Y Ono¹, F Calbaheu¹, JE Morgan², T Katagiri³, H Amthor⁴ and PS Zammit^{*1}

Satellite cells are the resident stem cells of adult skeletal muscle, supplying myonuclei for homeostasis, hypertrophy and repair. In this study, we have examined the role of bone morphogenetic protein (BMP) signalling in regulating satellite cell function. Activated satellite cells expressed BMP receptor type 1A (BMPR-1A/Alk-3) and contained phosphorylated Smad proteins, indicating that BMP signalling is operating during proliferation. Indeed, exogenous BMP4 stimulated satellite cell division and inhibited myogenic differentiation. Conversely, interfering with the interactions between BMPs and their receptors by the addition of either the BMP antagonist Noggin or soluble BMPR-1A fragments, induced precocious differentiation. Similarly, blockade of BMP signalling by siRNA-mediated knockdown of BMPR-1A, disruption of the intracellular pathway by either Smad5 or Smad4 knockdown or inhibition of Smad1/5/8 phosphorylation with Dorsomorphin, also caused premature myogenic differentiation. BMP signalling acted to inhibit the upregulation of genes associated with differentiation, in part, through regulating Id1. As satellite cells differentiated, Noggin levels increased to antagonise BMP signalling, since Noggin knockdown enhanced proliferation and impeded myoblast fusion into large multinucleated myotubes. Finally, interference of normal BMP signalling after muscle damage *in vivo* perturbed the regenerative process, and resulted in smaller regenerated myofibres. In conclusion, BMP signalling operates during routine satellite cell function to help coordinate the balance between proliferation and differentiation, before Noggin is activated to antagonise BMPs and facilitate terminal differentiation.

Cell Death and Differentiation advance online publication, 6 August 2010; doi:10.1038/cdd.2010.95

Muscle satellite cells are the resident stem cells of skeletal muscle and supply myonuclei for postnatal muscle growth, and for maintenance and repair in adult.¹ Satellite cells are located on the surface of myofibres and are mitotically quiescent in healthy adult muscle. In response to cues for routine myofibre homeostasis or hypertrophy, or the sporadic demands of muscle repair, satellite cells are activated to generate myoblasts that proliferate and eventually undergo myogenic differentiation to provide new myonuclei. Satellite cells also self-renew, thus maintaining a population of quiescent, undifferentiated precursors available to respond to repeated demand.^{2–4}

Satellite cell function is controlled by various regulatory pathways, chief amongst them being Notch/Delta and Wnt signalling.¹ Many of these same regulatory networks also control embryonic myogenesis, in addition to many other processes, both during development and repair in adult. Another important network for organising embryonic and foetal myogenesis involves the Bone morphogenetic proteins (BMPs). BMPs belong to the transforming growth factor- β

family and initiate signalling by binding to the transmembrane type 1 and type 2 BMP receptors (BMPRs). On BMP binding, type 1 and 2 receptors complex on the cell surface, allowing the constitutively active kinase of the type 2 receptor to transphosphorylate the type 1 receptor.⁵ This in turn phosphorylates the R-Smads – Smad1, Smad5 and Smad8 (pSmad1/5/8) – which translocate to the nucleus to regulate transcription of target genes including *Ids*.^{6–8} Inhibitor of differentiation/DNA-binding (Id) proteins (comprising Id1, 2, 3, 4) bind ubiquitously expressed E-proteins to form inactive heterodimers, thereby preventing the same E-proteins from binding with tissue-specific transcription factors such as MyoD and myogenin, a step necessary for their efficient function.⁹ BMP signalling can be modified in a number of ways, including through secreted antagonists such as Noggin, which bind BMPs with high affinity to interfere with interactions between BMPs and their receptors.⁵

Although crucial for bone and cartilage formation and repair,^{5,10} BMPs also inhibit myogenic differentiation to prevent ectopic myogenesis in the lateral plate mesoderm.

¹King's College London, Randall Division of Cell and Molecular Biophysics, New Hunt's House, Guy's Campus, London SE1 1UL, UK; ²Dubowitz Neuromuscular Centre, UCL Institute of Child Health, 30 Guilford Street, London WC1N 1EH, UK; ³Division of Pathophysiology, Research Centre for Genomic Medicine, Saitama Medical University, 1397-1 Yamane, Hidaka-shi, Saitama 350-1241, Japan and ⁴UPMC INSERM, UMR S 974/CNRS UMR 7215, Institut de Myologie, 105 bd de l'Hôpital, 75013 Paris, France

*Corresponding author: PS Zammit, King's College London, Randall Division of Cell and Molecular Biophysics, New Hunt's House, Guy's Campus, London SE1 1UL, UK. Fax: +44 207 848 6435; E-mail: peter.zammit@kcl.ac.uk

Keywords: satellite cell; BMP; Noggin; Smad; Id1; skeletal muscle

Abbreviations: BMP, bone morphogenetic protein; BMPR-1A, bone morphogenetic protein receptor type 1A/Alk-3; sBMPR-1A, soluble bone morphogenetic protein receptor 1A fragments; caBMPR-1A, constitutively active bone morphogenetic protein receptor type 1A; pSmad1/5/8, phosphorylated Smad1, Smad5 and Smad8; Id, inhibitor of differentiation/DNA-binding protein; FOP, Fibrodysplasia ossificans progressiva; EDL, extensor digitorum longus; MyHC, myosin heavy chain; CKM, Muscle creatine kinase; DAPI, 4,6-diamidino-2-phenylindole; T0, freshly isolated; T48, cultured for 48 h; T72, cultured for 72 h

Received 17.12.09; revised 14.6.10; accepted 15.6.10; Edited by R De Maria

In the dermomyotome, however, BMP signalling itself must be inhibited, to permit the onset of myogenesis.^{11–14} BMPs not only impede myogenic differentiation in immortalised myogenic cell lines (e.g., C2) and primary myogenic cells *in vitro* but also induce osteoblastic gene expression and differentiation towards the osteoblast lineage.^{15–18} Interestingly, although able to express early markers of osteogenic differentiation such as alkaline phosphatase, many primary myogenic cells also retain expression of proteins associated with myogenesis (e.g., Pax7 and MyoD) after exposure to BMPs for several days.^{15,17} As intramuscular injection of certain BMPs (e.g., BMP2 and BMP4) can lead to ectopic bone formation *in vivo*,^{19,20} these *in vitro* observations were thought to provide mechanistic insight into Fibrodysplasia ossificans progressiva (FOP), a rare disorder of skeletal malformations and progressive extra-skeletal ossification in muscle. FOP is caused by a mutation in *ALK-2*, which renders this BMPR type 1 (BMPR-1) constitutively active,¹⁹ and inhibition of this mutant *ALK-2* reduces ossification.²¹ However, Lounev *et al.*²⁰ have recently shown that few (<5%) muscle progenitors actually contribute to BMP-induced heterotopic ossification *in vivo*.

In this study, we investigated the role of BMP signalling in satellite cell function during adult myogenesis. During activation and proliferation, satellite cells robustly express BMPR-1A (Alk-3), with pSmad1/5/8 and Smad4 present in their nuclei, indicative of operational BMP signalling. Exogenous BMP4 can sustain satellite cell division and reduce differentiation, with BMP4 functioning through BMPR-1A. Conversely, antagonising the interaction of BMP with its receptors or perturbing intracellular BMP signalling by either inhibiting Smad1/5/8 phosphorylation or reducing Smad5 or Smad4 levels, all induced premature differentiation. Manipulation of BMP signalling affected Id1 levels: a known inhibitor of differentiation that regulates the function of the myogenic regulatory factors (that comprise of Myf5, MyoD, myogenin and MRF4) through sequestration of E-proteins. Satellite cell progeny then upregulate the BMP antagonist Noggin as they differentiate, and knockdown of Noggin enhanced proliferation and impeded differentiation. As blockade of BMP signalling after muscle injury hindered regeneration, our observations show that BMP signalling is a potent regulator of routine satellite cell function in adult.

Results

BMP pathway proteins are present in activated and proliferating satellite cells. Satellite cell function can be modelled *in vitro*. On stimulation by mitogen-rich medium (termed plating or proliferation medium here), isolated Pax7-expressing quiescent satellite cells are activated and upregulate MyoD. Satellite cells then proliferate, before either downregulating Pax7, maintaining MyoD, inducing myogenin and proceeding to differentiate, or downregulating MyoD and maintaining Pax7, to return to a quiescent-like state, modelling self-renewal.^{2,3}

To first determine the expression profile of BMPR-1A, we immunostained satellite cells retained in their niche on myofibres isolated from the extensor digitorum longus (EDL)

muscle. BMPR-1A was undetectable in the vast majority of quiescent satellite cells on freshly isolated (T0) myofibres (Figure 1a). However, after culturing in plating medium for 48 (T48) or 72 h (T72), BMPR-1A became robustly expressed in activated and proliferating satellite cells (Figure 1a). *BMPR-1B* was not detectable by Q-PCR (data not shown), consistent with its absence in C2C12 myoblasts.²² Intracellular BMP signalling through BMPR-1A operates by phosphorylation of the carboxyl terminal of R-Smad proteins. Immunostaining for either pSmad1/5/8 or Smad5, revealed a strong nuclear signal in activated and proliferating (T48 and T72), but not quiescent (T0), satellite cells (Figure 1b and c). The common-mediator Smad (Co-Smad) Smad4, which facilitates translocation of Smad1/5/8 to the nucleus and promotes their transcriptional activity,⁵ was also present in the nuclei of activated satellite cells (Figure 1c). Thus, the expression dynamics of BMPR-1A, pSmad1/5/8, Smad4 and Smad5 mirror each other, and indicate that BMP signalling is operating in activated and proliferating satellite cells.

As Noggin-mediated BMP antagonism contributes to initiation of the myogenic programme during embryogenesis,¹³ we hypothesised that Noggin may also modify BMP signalling in satellite cells. Noggin was undetectable in quiescent (T0), and at low levels in activated Pax7⁺, satellite cells (Figure 2a and b). In contrast, Noggin was highly expressed by differentiating myoblasts at T72, as shown by co-immunostaining for Noggin and myogenin (Figure 2b). Culturing satellite cells attached to a myofibre provides a useful model for studying satellite cell activation, proliferation and the initial stages of differentiation. Later events, such as myoblast fusion into large multi-nucleated myotubes, however, are better studied in satellite cells isolated from their associated myofibre and plated onto Matrigel-coated culture dishes. Such plated satellite cell-derived myoblasts cultured in differentiation medium for 2 days clearly exhibited high Noggin levels in myotubes and other Pax7⁻ cells (Figure 2c and d).

BMP regulates the balance between proliferation and differentiation in satellite cells. We next examined the effects of stimulating BMP signalling, and used administration of recombinant BMP4 to achieve this, as it is present in serum.²³ Addition of recombinant BMP4 protein (100 ng/ml) to EDL satellite cells retained in their niche on the myofibre significantly increased the number of Pax7⁺MyoD⁺ satellite cells, but decreased the number of cells with the differentiating Pax7⁻MyoD⁺ phenotype (Figure 3a). Inhibition of differentiation by BMP4 was confirmed by co-immunostaining for myogenin and Pax7 (Figure 3b). Plating medium contains chick embryo extract and horse serum, hence is rich in growth factors, and also contains BMP4.²³ Under these culture conditions, satellite cell proliferation is likely to be near maximal; hence, addition of BMP4 did not further increase cell division (Figure 3a and b). As satellite cells retained expression of genes associated with myogenesis, these short exposures to BMP4 did not induce any obvious loss of myogenic identity.

To interfere with BMP binding to its receptors, we added recombinant Noggin protein (50 ng/ml) or soluble BMPR-1A fragments (sBMPR-1Af; 200 ng/ml) to cultures of satellite cells associated with a myofibre for 72 h. Exposure to either Noggin

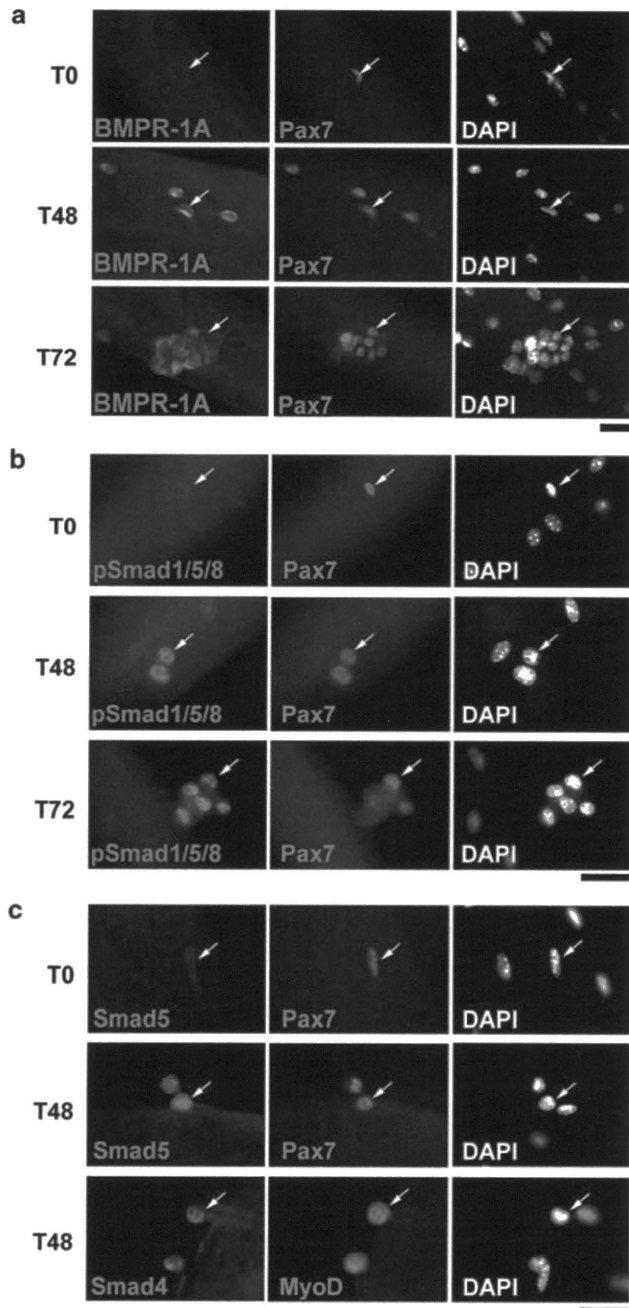


Figure 1 BMPR-1A, pSmad 1/5/8, Smad4 and Smad 5 are upregulated during satellite cell activation. Isolated EDL myofibres with their associated satellite cells were either immediately fixed (T0) or cultured in plating medium for either 48 h (T48) or 72 h (T72) before fixation and immunostaining. (a) BMPR-1A was undetectable on the majority of Pax7⁺ quiescent cells at T0, but robustly expressed in both Pax7⁺ and Pax7⁻ cells at both T48 and T72. (b) Quiescent Pax7⁺ satellite cells (T0) did not contain pSmad1/5/8, whereas pSmad1/5/8 became readily detectable in the nuclei of proliferating Pax7⁺ cells at T48, and both Pax7⁺ and Pax7⁻ cells at T72. (c) In accordance with the dynamics of pSmad1/5/8 expression, Smad5 levels were very low/absent in quiescent satellite cells at T0, but upregulated in both proliferating Pax7⁺ and MyoD⁺ cells at T48, as was Smad4. Arrows indicate the same satellite cell at each time point to aid comparison. Representative images from at least three independent experiments are shown. Scale bar equals 30 μ m

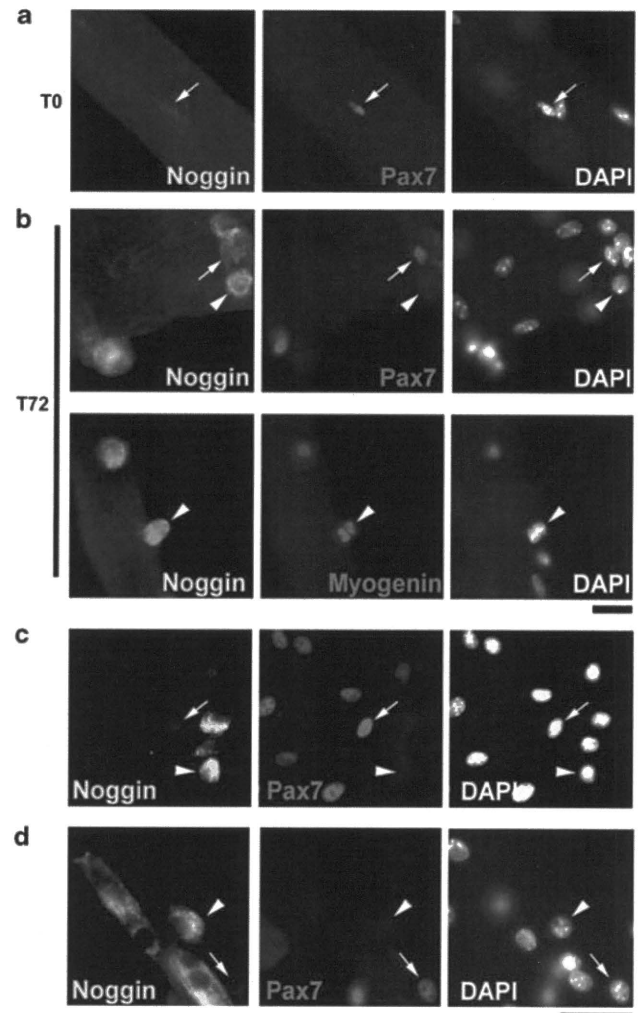


Figure 2 Noggin is highly expressed in satellite cell progeny committing to myogenic differentiation. Isolated EDL myofibres with their associated satellite cells were either immediately fixed (T0) or cultured in plating medium for 72 h (T72) before fixation and immunostaining. (a) Noggin was not expressed in quiescent Pax7⁺ satellite cells (arrows) at T0. (b) After culture, Noggin was highly expressed in both Pax7⁻ and Myogenin⁺ cells committed to myogenic differentiation (arrowheads) at T72, but at much lower levels in Pax7⁺ cells (arrows). (c and d) Plated satellite cell-derived myoblasts were cultured in differentiation medium for 2 days and immunostained for Noggin and Pax7. (c) Pax7⁻ differentiating cells (arrowheads) and (d) myotubes both expressed high levels of Noggin protein, while Noggin levels in Pax7⁺ cells were low (arrows). Representative images from at least three independent experiments are shown. Scale bar equals 30 μ m

or sBMPR-1Af resulted in a significant reduction in the mean total satellite cell number per myofibre, particularly of cells with the Pax7⁺MyoD⁺ phenotype (Figure 3a). Numbers of differentiating Pax7⁻MyoD⁺ cells were already increased at T48, and became the predominant phenotype at T72, signifying a precocious onset of differentiation (Figure 3a). There were also significantly fewer self-renewing Pax7⁺MyoD⁻ cells present at T72 (Figure 3a). Co-immunostaining for Pax7 and myogenin confirmed that both Noggin and sBMPR-1Af enhanced differentiation, revealing a significant increase in cells with the Pax7⁻myogenin⁺

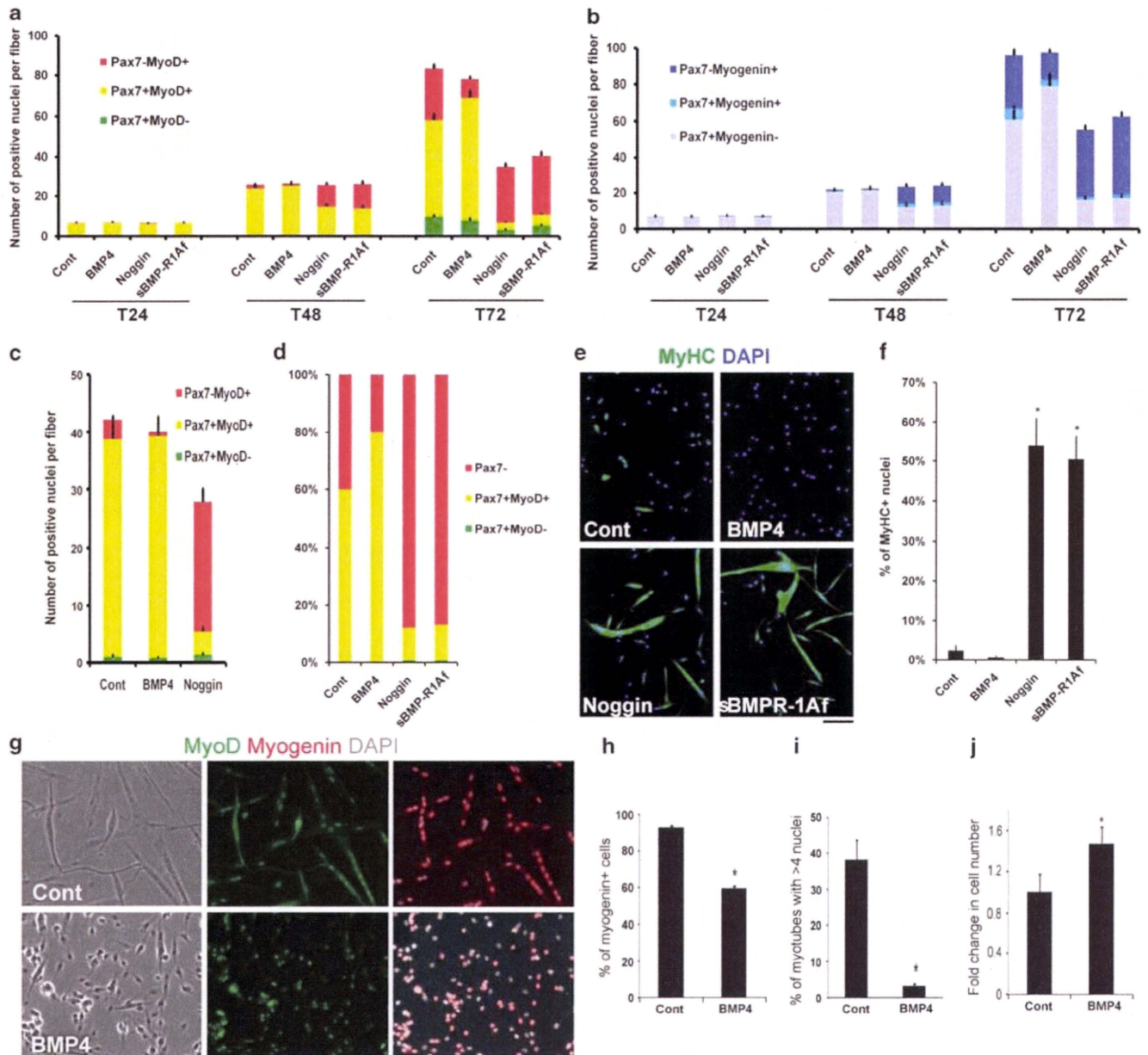


Figure 3 Inhibition of BMP signalling promotes myogenic differentiation in satellite cells. Isolated myofibres associated with satellite cells, or plated satellite cell-derived myoblasts, were cultured in the presence of recombinant BMP4 protein (100 ng/ml), recombinant Noggin protein (50 ng/ml) or sBMPR-1Af (200 ng/ml). (a) EDL myofibres were cultured in plating medium supplemented with BMP4, Noggin or sBMPR-1Af, then fixed after 24 (T24), 48 (T48) or 72 (T72) h and immunostained for Pax7 and MyoD. BMP4 reduced the number of Pax7⁺MyoD⁺ cells. Both Noggin and sBMPR-1Af reduced the mean total number of cells per myofibre and promoted myogenic differentiation (increase of the Pax7⁻MyoD⁺ phenotype). (b) Co-immunostaining isolated myofibres for Pax7, and myogenin confirmed that BMP4 inhibited myogenic differentiation, whereas Noggin and sBMPR-1Af promoted it, as shown by the increase of satellite cell progeny with the Pax7⁻myogenin⁺ phenotype. (c) Treatment of masseter-derived satellite cells with BMP4 or Noggin for 72 h produced the same result as for EDL cells, that is, BMP4 inhibited, whereas Noggin induced, myogenic differentiation. (d–f) To examine the effects of these recombinant proteins on the later stages of myogenesis, EDL satellite cells were plated and cultured in the presence of recombinant BMP4, Noggin or sBMPR-1Af in plating medium for 4 days (with the medium changed every other day). (d) Co-immunostaining for Pax7 and MyoD again showed a dramatic increase in the proportion of cells with the differentiating Pax7⁻ phenotype when exposed to either Noggin or sBMPR-1Af. (e, quantified in f) Immunostaining for MyHC revealed that exposure to either Noggin or sBMPR-1Af resulted in precocious differentiation and formation of large multi-nucleated myotubes. (g–j) To better examine the effects of BMP on satellite cell proliferation and myogenic progression, plated satellite cells were also cultured in differentiation medium supplemented with recombinant BMP4 protein (200 ng/ml) and immunostained for MyoD and myogenin (g, quantified in h–j). Exposure to BMP4 significantly reduced the proportion of cells expressing myogenin (h) and fusing into large myotubes (i), but stimulated continued cell proliferation, resulting in a 1.46 ± 0.2 -fold increase in total cell number (j). Data are mean \pm S.E.M. (a–c) or mean \pm S.D. (f–j) from at least three independent experiments. Asterisk indicates that data are significantly different from controls ($P < 0.05$) using Student's *t*-test. Scale bar equals 100 μ m for e

phenotype (Figure 3b). These effects were not restricted to satellite cells from somite-derived muscles, as those from the branchiomeric masseter muscle, which has a different

embryonic origin,²⁴ also exhibited fewer differentiating Pax7⁻MyoD⁺ cells in the presence of BMP4, but increased differentiation when exposed to Noggin (Figure 3c).

Culture in proliferation medium does not readily support differentiation of plated satellite cells. Addition of recombinant BMP4 resulted in a higher proportion of cells co-immunostained for Pax7 and MyoD (Figure 3d). The differentiation index under these culture conditions, however, is already so low that any inhibitory effect of BMP4 on formation of myosin heavy chain (MyHC) containing myocytes was not significant (Figure 3e, quantified in f). Addition of either Noggin or sBMPR-1Af, however, triggered a robust differentiation, as shown by both the reduced proportion of plated cells with Pax7 (Figure 3d) and the marked increase in myotubes containing MyHC (Figure 3e and f). The proportion of satellite cell progeny with the self-renewing Pax7⁺MyoD⁻ phenotype was also significantly increased, from effectively zero in control cultures to ~0.7% after exposure to either Noggin or sBMPR-1Af (Figure 3d).

Finally, we determined the effects of exogenous BMP4 on satellite cells after serum deprivation, which normally promotes myogenin expression, cell cycle exit and fusion into myotubes. However, addition of recombinant BMP4

(200 ng/ml) to differentiation medium led to a significant drop in the proportion of cells containing myogenin (Figure 3g, quantified in h) and fusing into myotubes (Figure 3g, quantified in i). On the other hand, MyoD remained readily detectable in the nuclei of these cells after exposure to BMP4 for 2 days (Figure 3g). Importantly, BMP4 caused a 1.46 ± 0.2 -fold increase in total cell number, indicating that BMP4 not only inhibits differentiation but also stimulates satellite cell proliferation, despite serum depletion (Figure 3j).

BMP operates through BMPR-1A to prevent precocious differentiation. To determine whether BMP signalling was transduced through BMPR-1A in activated satellite cells, we used siRNA-mediated knockdown,²⁵ which reduced the mean total number of satellite cells per myofibre when assayed at T72 (Figure 4a, quantified in b). In particular, BMPR-1A knockdown significantly decreased the number of both Pax7⁺MyoD⁺ cells and Pax7⁺MyoD⁻ self-renewed cells, but not the number of Pax7⁻MyoD⁺ differentiating cells, which became the predominant phenotype (Figure 4b).

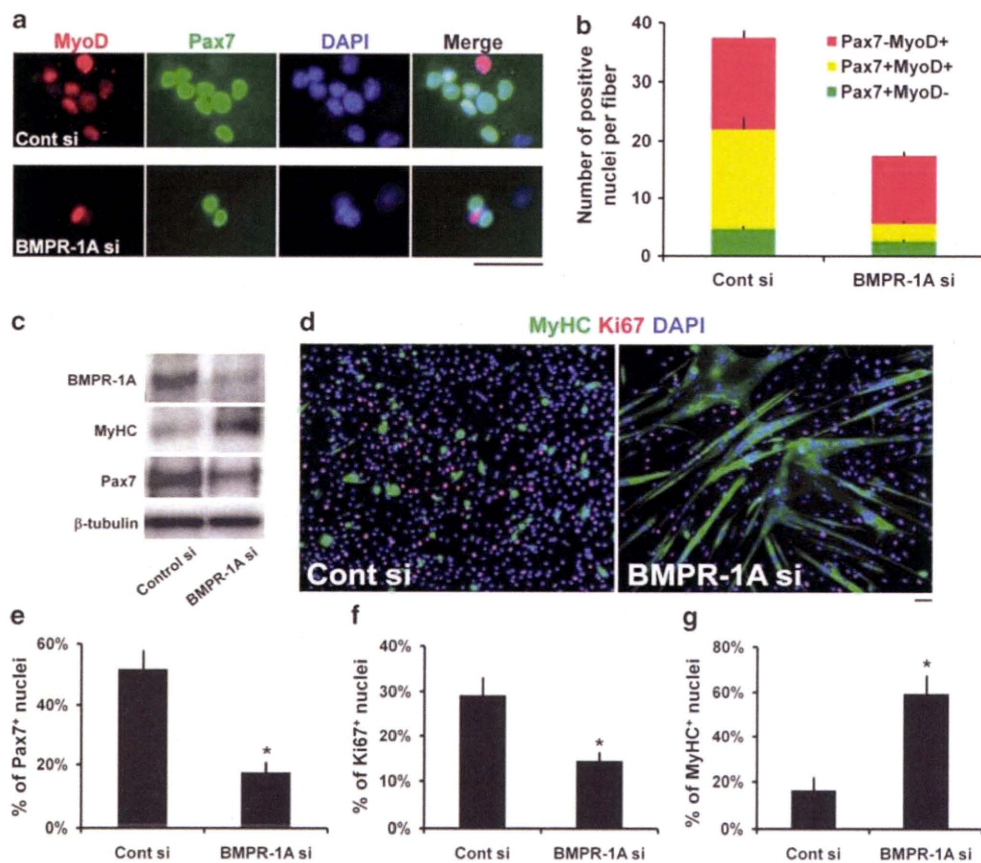


Figure 4 BMP signalling functions through BMPR-1A. We used siRNA-mediated protein knockdown to explore whether BMP signalling operates through BMPR-1A. (a, quantified in b) Control (Cont si) or BMPR-1A (BMPR-1Asi) siRNA were transfected into satellite cells retained in their niche on isolated EDL myofibers and cultured for ~2.5 days before fixation and co-immunostaining for Pax7 and MyoD. BMPR-1A knockdown reduced the mean total number of cells, especially the number of Pax7⁺MyoD⁺ cells. (c–g) Control siRNA or BMPR-1A siRNA duplexes were also transfected into plated satellite cell-derived myoblasts. (c) Immunoblot analysis clearly demonstrated efficient knockdown of BMPR-1A protein levels, which resulted in an upregulation of MyHC, but a downregulation of Pax7 (β -tubulin served as a protein loading control). (d, quantified in e–g) The effects of BMPR-1A knockdown were also examined by immunostaining for Pax7, Ki67 or MyHC in plated satellite cell-derived myoblasts cultured in proliferation medium for 3 days after transfection. (d) Representative images of Ki67 and MyHC immunostaining show that BMPR-1A knockdown inhibited cell proliferation and promoted myogenic differentiation. (e and f) There was a significant decrease in the proportion of cells containing Pax7 or Ki67 (proliferating) after BMPR-1A siRNA-transfection. (g) In contrast, there was a significant increase in the proportion of MyHC⁺ differentiated cells and myotubes. Data are either mean \pm S.E.M. (b) or mean \pm S.D. (e–g) from at least three independent experiments. Asterisk denotes that data are significantly different from control ($P < 0.05$). Scale bar equals 50 μ m

The efficient reduction in BMPR-1A levels by siRNA was confirmed by western blot analysis of plated satellite cells, which also revealed decreased Pax7 levels, but an increase in the amount of MyHC (Figure 4c). Immunostaining (Figure 4d, quantified in e–g) confirmed that reducing BMPR-1A led to a reduction in the proportion of Pax7⁺ cells (Figure 4e), which was accompanied by a significant reduction in Ki67⁺ proliferating cells (Figure 4d and f). In contrast, there was an increase in the proportion of MyHC⁺ differentiated cells after BMPR-1A knockdown (Figure 4d and g).

Blockade of intracellular BMP signalling promotes myogenic differentiation. We next analysed the pSmad1/5/8 signalling cascade.⁵ The protein kinase inhibitor Dorsomorphin is a specific inhibitor of Smad1/5/8 phosphorylation by BMPRs.²⁶ Dorsomorphin (1–5 μ M) was not toxic to plated satellite cells, as shown using the TUNEL assay (data not shown). Exposure of cultured myofibres to Dorsomorphin significantly decreased the mean number of associated Pax7⁺MyoD⁺ satellite cells, and hence Pax7⁻MyoD⁺ differentiating cells became the main phenotype (Figure 5a). Dorsomorphin also induced myogenic differentiation in a dose-dependent (0.1–1.0 μ M) manner in plated satellite cells maintained in proliferation medium (Figure 5b). Additionally, we also targeted Smad signalling using siRNA-mediated knockdown of Smad5 or Smad4, which effectively reduced the levels of the translated protein (Figure 5c and d). Co-immunostaining for Ki67 and MyHC revealed that Smad5 or Smad4 knockdown significantly reduced cell proliferation and induced precocious differentiation (Figure 5e, quantified in f and g).

BMP signalling regulates the ability of MyoD to activate its transcriptional targets. To understand how interference with BMP signalling promotes myogenic differentiation, we investigated Id1, a downstream target of BMPs^{6–8} and a negative controller of MyoD and myogenin.^{9,27} We recently showed that Id1 is highly expressed in proliferating satellite cells, before being downregulated during myogenic differentiation.²⁵ Immunostaining showed that exposure to Dorsomorphin to inhibit Smad1/5/8 phosphorylation reduced Id1 levels in both satellite cells retained in their niche on the myofibre (Figure 6a) and in plated satellite cells (Figure 6b).

Muscle creatine kinase (*CKM*) is a well-characterised gene and provides a useful tool to quantify both the ability of MyoD to transactivate its target genes, and myogenic differentiation.²⁷ Therefore, we measured the activity of a *CKM-luciferase* construct (*CKM-LUCpCS2*) in response to both exogenous Id1 and perturbation of BMP signalling (Figure 6c). As expected, *CKM-LUCpCS2* activity was significantly decreased after transfection with *Id1* (Figure 6c). Importantly, transfection of a plasmid encoding a constitutively active BMPR-1A (caBMPR-1A) that phosphorylates Smad1/5/8 in the absence of BMP ligands²⁸ also significantly reduced *CKM-LUCpCS2* activity (Figure 6c). In contrast, inhibition of Smad1/5/8 phosphorylation with Dorsomorphin significantly increased the activity of *CKM-LUCpCS2*, but Id1 was able to completely reverse this Dorsomorphin-mediated increase (Figure 6c). Finally, caBMPR-1A also reduced

CKM-LUCpCS2 activity back to control levels, despite the presence of Dorsomorphin (Figure 6c). Thus, BMP signalling in satellite cells acts to limit the transcriptional activation of genes controlled by MyoD and enhanced during differentiation.

Noggin antagonises BMPs to facilitate myogenic differentiation. Noggin is upregulated as satellite cells differentiate (Figure 2). To examine the role of Noggin, we first performed siRNA-mediated knockdown in plated satellite cells, and immunostaining showed that it worked efficiently (Figure 7a). Plated satellite cells transfected with Noggin siRNA and co-immunostained for Ki67 and MyHC (Figure 7b, quantified c–e) had a significantly increased proportion of proliferating Ki67⁺ satellite cells (Figure 7c). However, the proportion of differentiating MyHC⁺ cells and the fusion index were both markedly reduced, with only myocytes or small myotubes present (Figure 7b and e). Consistent with these observations, western blot analysis revealed a slight decrease in myogenin levels (Figure 7f). We also found that the fusion defect induced by Noggin knockdown could be rescued by Dorsomorphin-mediated blockade of intracellular BMP signalling (Figure 7g, quantified h), indicating that endogenous Noggin from differentiating cells is required for proper myotube formation, through suppression of BMP signalling.

BMP signalling is operative during muscle regeneration *in vivo*. Finally, we evaluated whether BMP signalling was also operative in satellite cells in regenerating muscle *in vivo*. Cardiotoxin was used to induce damage in the gastrocnemius muscle of adult mice. After 3 days, the regenerating muscles were removed, cryosectioned and immunostained for pSmad1/5/8, together with MyoD, to identify satellite cell-derived myoblasts: 97.4 \pm 2.9% (n = 50 cells from each of 3 mice) of MyoD⁺ cells contained pSmad1/5/8 (Figure 8a). Undamaged areas of the muscle periphery provided the control and no pSmad1/5/8 immunostaining was associated with myofibres in these non-regenerating regions (data not shown).

Regenerating gastrocnemius muscle was also injected with either 50 μ l of 10 μ M Dorsomorphin (Figure 8b–d) or 50 μ l of 100 μ g/ml sBMPR-1A (Figure 8e–g) at 1 and 3 days after cardiotoxin-induced injury. The contralateral regenerating muscle served as the control and was injected with 50 μ l of vehicle. Regenerating muscles were removed on day 8 and immunostained for MyHC and collagen type 1 (Figure 8b and e). Administration of Dorsomorphin resulted in a significant \sim 20% decrease in the mean perimeter of centrally nucleated regenerating myofibres compared with controls, whereas the reduction was nearer \sim 40% with sBMPR-1A (Figure 8c and f). A significant \sim 1.5-fold increase in collagen type 1 deposition after either Dorsomorphin or sBMPR-1A administration was also observed (Figure 8d and g).

Discussion

In this study, we investigated the role of BMP signalling in normal adult myogenesis. We found that exogenous BMP4 was able to sustain proliferation in satellite cells and inhibit differentiation. Conversely, blocking interaction of BMP with

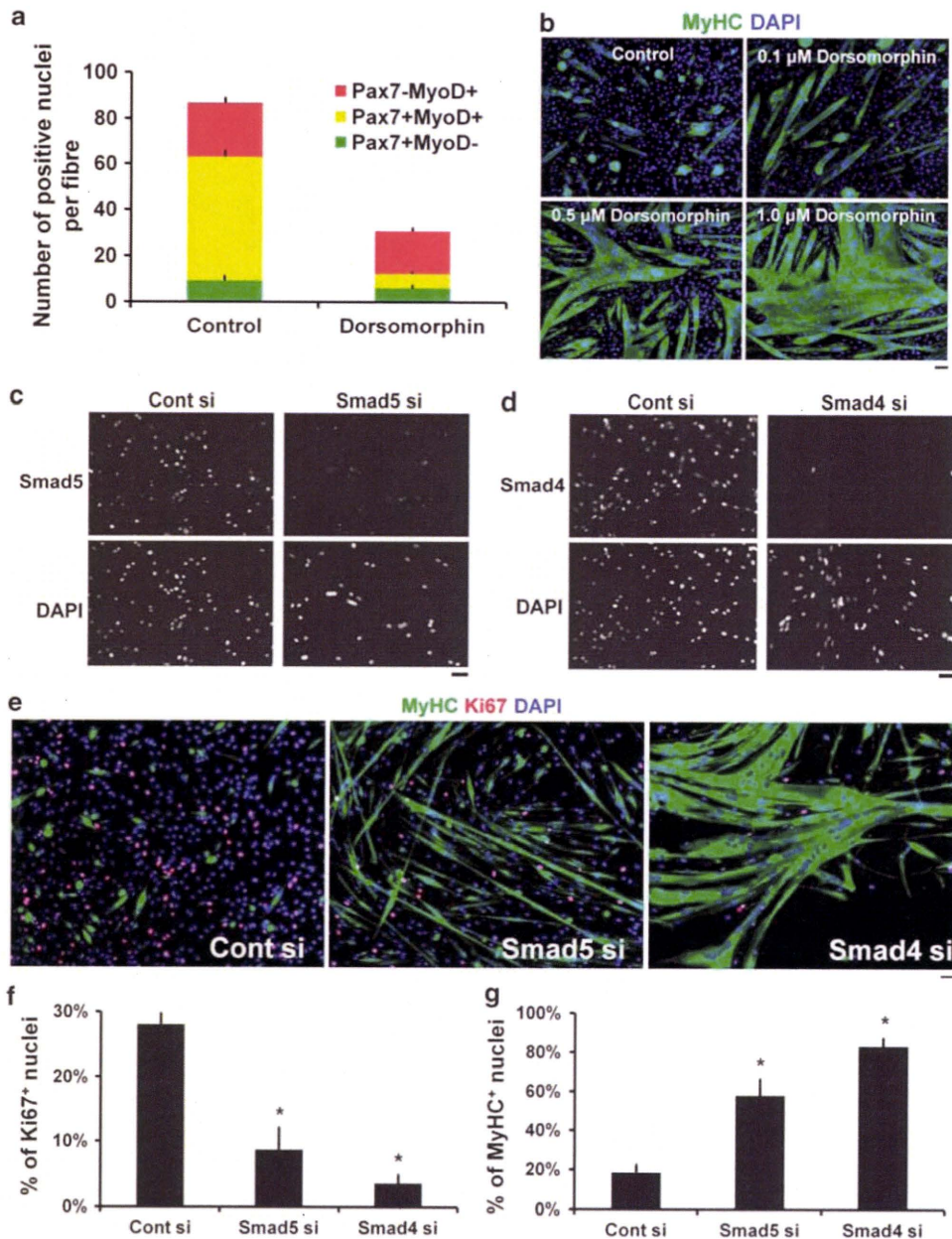


Figure 5 Inhibiting intracellular BMP signal mediation promotes myogenic differentiation. To inhibit BMP signaling, we used either Dorsomorphin, an inhibitor of Smad1/5/8 phosphorylation, or siRNA to knockdown the R-Smad, Smad5, or Co-Smad, Smad4, levels. (a) EDL myofibres and their associated satellite cells were cultured with or without 1 μM Dorsomorphin and the plating medium changed daily. Dorsomorphin markedly decreased the mean total number of cells per fibre, particularly the number of cells with the Pax7⁺MyoD⁺ phenotype. (b) Satellite cell-derived myoblasts were plated at high cell density (80–90% confluency) and cultured in proliferation medium for 2 days with or without Dorsomorphin. Immunostaining for MyHC showed that Dorsomorphin promoted myogenic differentiation and fusion in a dose-dependent manner. (c and d) Efficient siRNA-mediated knockdown of Smad5 or Smad4 was confirmed by immunostaining of plated satellite cells 24 h after transfection. (e, quantified in f and g) Co-immunostaining for MyHC and Ki67 after Smad5 or Smad4 silencing for 3 days in proliferation medium was sufficient to promote cell cycle exit and induce precocious differentiation, characterised by a decreased proportion of cells with Ki67⁺ expression and an increase in MyHC⁺ cells and myotubes. Data are mean ± S.E.M. (a) or mean ± S.D. (f and g) from at least three independent experiments. Asterisk indicates that data are significantly different from control conditions ($P < 0.05$). Scale bar equals 50 μm

its receptors, downregulating BMPR-1A or perturbing intracellular BMP signal mediation, all induced rapid differentiation. Thus, BMP signalling initially serves to allow expansion of the satellite cell pool by stimulating proliferation and preventing precocious myogenic differentiation (Figure 9).

The source of BMPs that act on satellite cells *in vivo* remains to be determined, but myogenic cells can express

and secrete BMP4,^{29,30} with higher levels produced by myoblasts from dystrophic muscle.³¹ Additionally, muscle damage may also expose satellite cells to BMP4 in serum,²³ and/or from cells such as macrophages, as microglia/macrophages produce BMPs after CNS damage.³² Although prolonged exposure of myogenic cells to high levels of BMPs can induce expression of various osteogenic genes,¹⁶ we

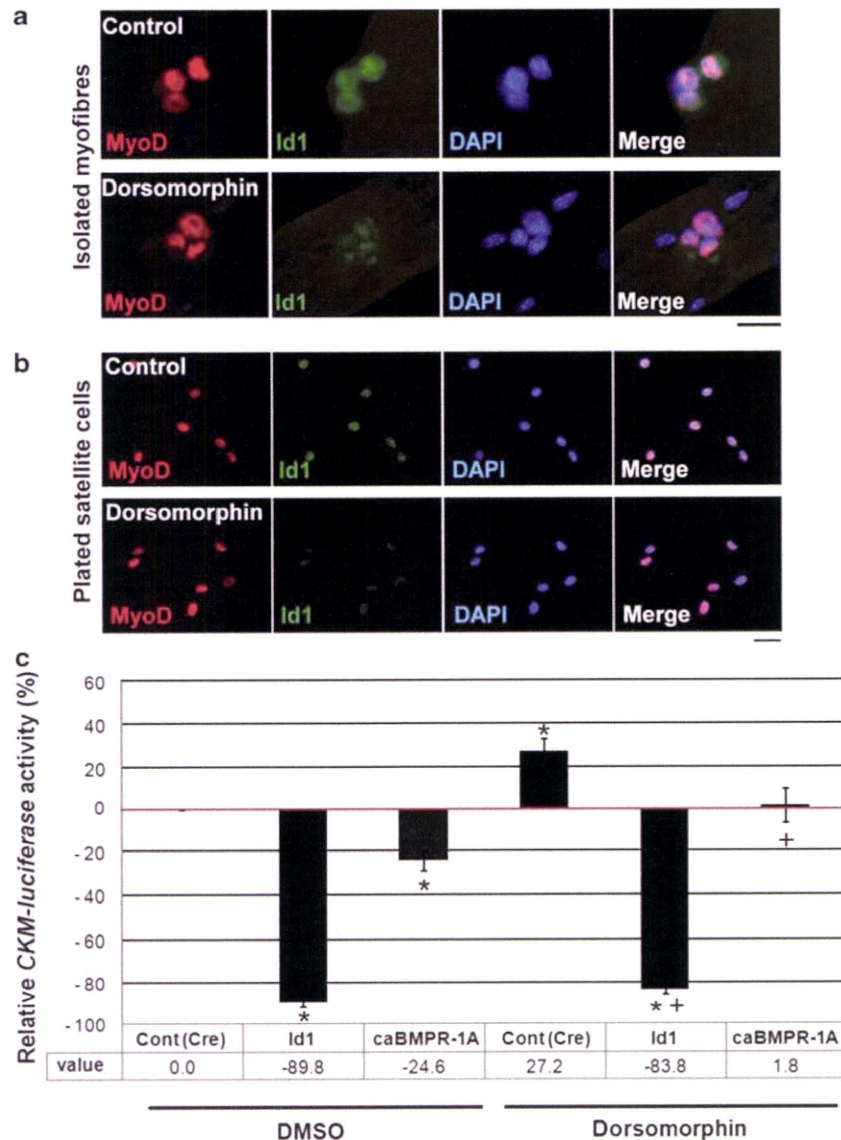


Figure 6 BMP signalling regulates the MyoD-controlled *CKM* promoter. Id1 is a target gene of BMP signalling and a negative regulator of MyoD activity. (a) Exposure to 3 μ M Dorsomorphin for 6 h to inhibit BMP signalling resulted in a downregulation of Id1 expression in satellite cells associated with a myofibre. (b) Similarly, immunostaining of plated satellite cells after exposure to 3 μ M Dorsomorphin for 18 h in proliferation medium also resulted in downregulation of Id1 protein. Scale bar equals 20 μ m. (c) To investigate the ability of MyoD to activate its transcriptional targets, plated satellite cell-derived myoblasts were transfected with a *CKM* (muscle creatine kinase) Luciferase reporter plasmid (*CKM-LUCpCS2*), whose activity is regulated by MyoD, together with a *Renilla* luciferase plasmid *pRL* driven by a minimal *tk* promoter, as an internal control. Plated satellite cells were co-transfected with either *Cre*-expressing control plasmid or *Id1*-expressing plasmid or constitutively active *BMPR-1A* (*caBMPR-1A*)-expressing plasmid, together with *CKM-LUCpCS2*. After transfection, the cells were cultured in proliferation medium with or without 5 μ M Dorsomorphin for 24 h before reporter assay. Id1 or *caBMPR-1A* reduced *CKM-LUCpCS2* activity. In contrast, inhibition of BMP signalling with Dorsomorphin had the opposite effect, and increased *CKM-LUCpCS2* activity. Both Id1 and *caBMPR-1A* were able to reverse this increase in *CKM-LUCpCS2* activity produced by exposure to Dorsomorphin. Data are represented as mean \pm S.D. from at least three independent experiments. Asterisk denotes that data are significantly different from control conditions, whereas a cross indicates that data are different from the level of *CKM-LUCpCS2* activity in the presence of Dorsomorphin ($P < 0.05$), using Student's *t*-test

found that satellite cells exposed to BMP4 for shorter periods, likely encountered during muscle repair/regeneration *in vivo*, did not obviously compromise their myogenic identity.

Satellite cells respond to BMPs because they express *BMPR-1A*, which was undetectable on most quiescent satellite cells, but upregulated as cells were activated. An early event in satellite cell activation is induction of MyoD, which can bind to the promoter of *BMPR-1A* to enhance its expression, and MyoD overexpression leads to *BMPR-1A*

induction.³³ Thus upregulation of *BMPR-1A* is part of the response of satellite cells to serum stimulation, and siRNA-mediated knockdown of *BMPR-1A* induced premature differentiation, showing that BMP signalling operates through *BMPR-1A*. Consistent with our observations, a dominant-negative *BMPR-1A* mutant enhanced myogenic differentiation in C2 cells maintained in high-serum medium, but a dominant-negative *BMPR-1B* mutant did not.²³ In contrast, we found that a *caBMPR-1A*²⁸ reduced the activity of a *CKM*

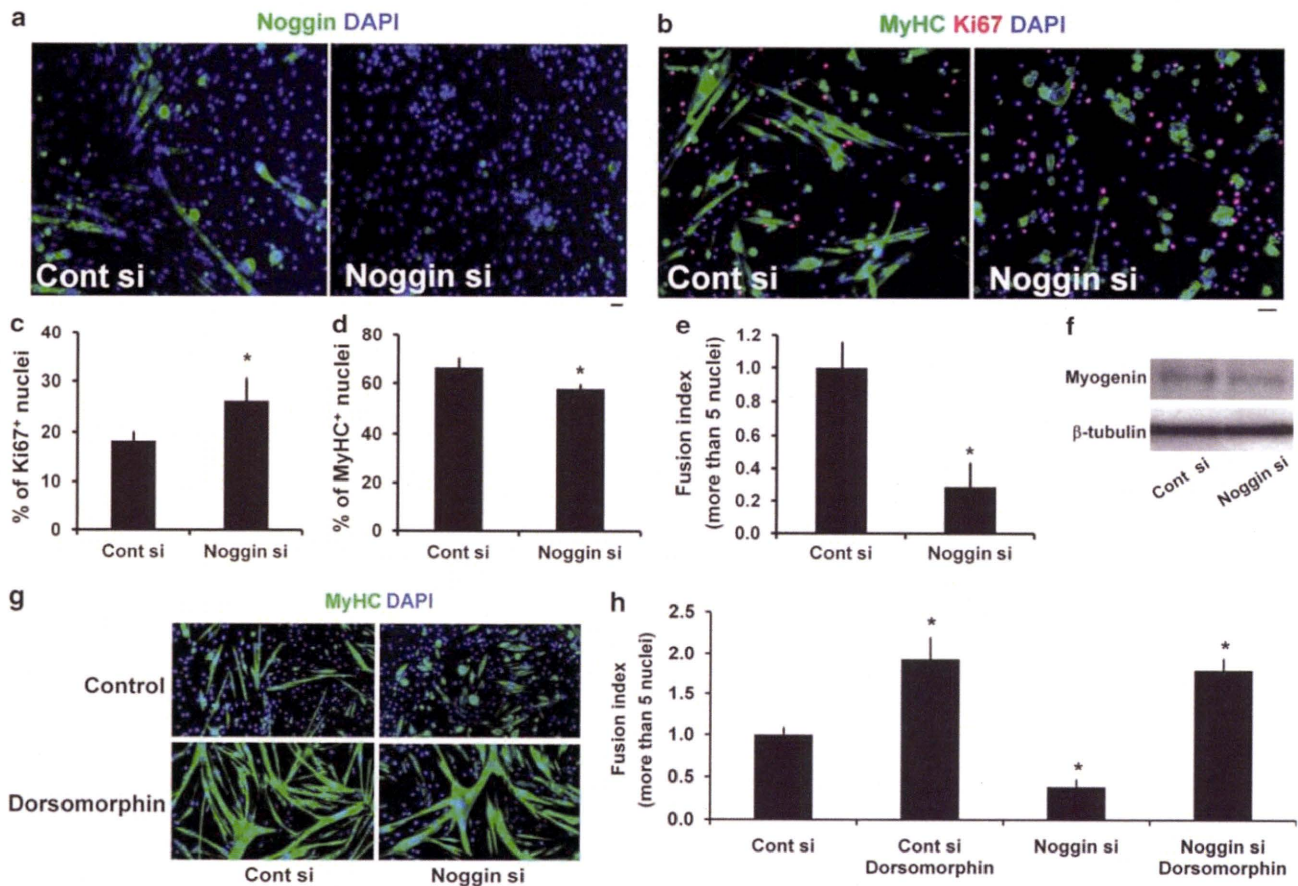


Figure 7 Reducing Noggin levels enhances satellite cell proliferation but inhibits differentiation. To further understand the role of Noggin in myogenic progression, we used siRNA-mediated knockdown of Noggin protein. (a) Efficient Noggin knockdown in plated satellite cell-derived myoblasts was confirmed by immunostaining for Noggin 3 days after siRNA (Noggin si) transfection. (b, quantified in c–e) The effects of Noggin knockdown were analysed by co-immunostaining for MyHC and Ki67, which revealed an increase in myoblast proliferation, but a reduction in differentiation and fusion into large myotubes. (f) Western blotting also showed that Noggin siRNA reduced myogenin levels in plated satellite cells. (g, quantified in h) The effect of Dorsomorphin (1 μ M) treatment to inhibit BMP signalling on Noggin siRNA-transfected cells was analysed by immunostaining for MyHC. Dorsomorphin reversed the fusion defect induced by Noggin knockdown. Mean \pm S.D. from at least three independent experiments is shown. Asterisk indicates that data are significantly different from control ($P < 0.05$) using paired one-tail *t*-test. Scale bar equals 30 μ m

reporter that is normally upregulated during myogenic differentiation.

BMPs are known to control the ability of MyoD to transactivate its target genes by Smad-mediated regulation of Id proteins,^{6–8} negative regulators of MyoD function and terminal differentiation.^{9,27} Proliferating satellite cell-derived myoblasts contain both MyoD and Id1, with Id1 presumably curtailing MyoD function to prevent premature differentiation. Id1 levels are then dramatically reduced as satellite cells undergo differentiation.²⁵ Consistent with these observations, although Id1 and Id3 are undetectable in muscle lysates from uninjured muscle, they are upregulated during muscle regeneration, peaking around day 3.³⁰ In satellite cells, we found that inhibiting BMP signalling reduced Id1 levels, promoted differentiation and increased *CKM* promoter activity.

Delta/Notch signalling permits satellite cell expansion and prevents precocious differentiation.³⁴ Notch signalling is required for BMP4 to impede myogenic differentiation in C2 cells: inhibitors of γ -secretase prevent cleavage of Notch to release the active intracellular domain and can partially reverse the BMP-induced differentiation block.¹⁸ The catalytic

subunit of the γ -secretase complex is presenilin-1, and we recently showed that presenilin-1 can inhibit satellite cell differentiation through both γ -secretase-dependent and γ -secretase-independent mechanisms.²⁵ The γ -secretase-dependent effects of presenilin-1 on impeding differentiation are likely through controlling Notch signalling. Crucially, however, the γ -secretase (Notch)-independent presenilin-1 mechanism operates by augmenting Pax7 and controlling Id1 levels,²⁵ and intriguingly, Id1, Id2 and Id3 are direct transcriptional targets of Pax7.²⁹ This γ -secretase-independent mechanism is unlikely to work through BMP signalling, however, as there is no difference in pSmad1/5/8 levels between *presenilin-1*-null or control embryonic fibroblasts transfected with MyoD, even though only the MyoD-expressing *presenilin-1*-null cells readily differentiate in high-serum medium (unpublished observations). Furthermore, overexpression of Wnt3a in C2 cells is capable of overcoming the BMP2-mediated block of differentiation by downregulating Id1.³⁵ Thus γ -secretase-independent presenilin-1 signalling and the BMP pathway both seem to separately converge on Ids to regulate satellite cell function.

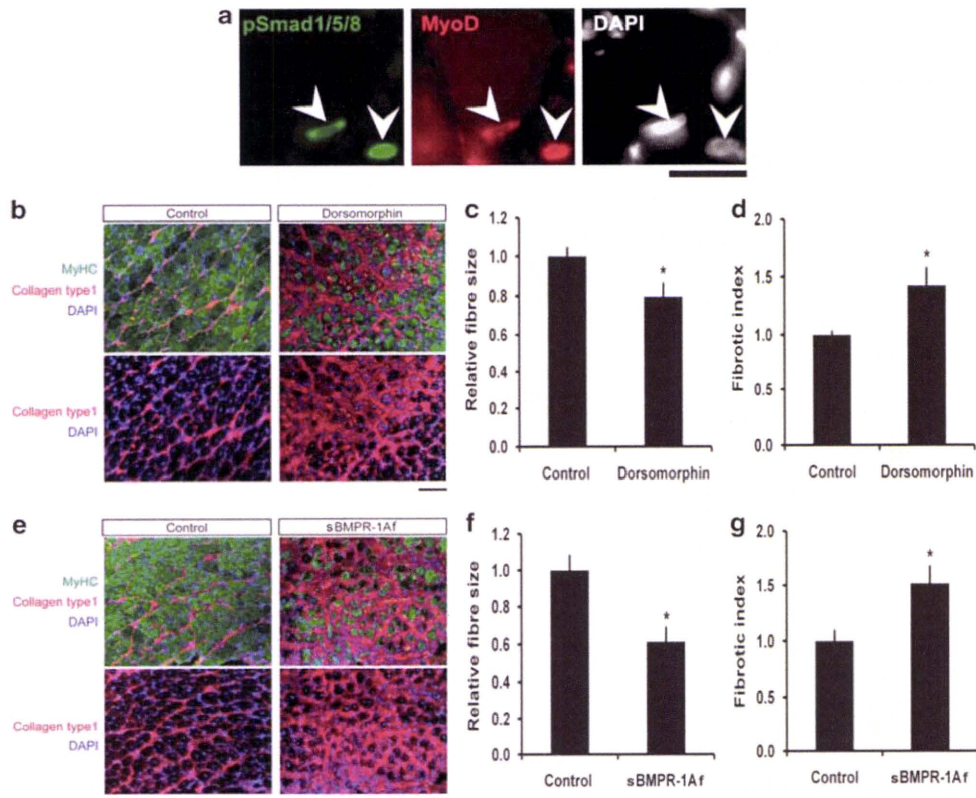


Figure 8 BMP signalling operates during normal muscle regeneration *in vivo*. Regeneration was induced in mouse gastrocnemius muscles by injection of cardiotoxin. (a) Satellite cell-derived myoblasts, identified by MyoD expression, also expressed pSmad1/5/8 (arrowheads) in regenerating muscle on day 3 of regeneration. (b–g) To examine the effects of blockade of BMP signalling, 50 μ l of 10 μ M Dorsomorphin/DMSO in saline or 50 μ l of 100 μ g/ml sBMPR-1Af were intramuscularly injected into the right gastrocnemius, 1 and 3 days after cardiotoxin injection. Regenerating left gastrocnemius served as a control and received vehicle alone (DMSO/saline for Dorsomorphin or BSA solution for sBMPR-1Af). Muscle regeneration was assayed by immunostaining cryosections for MyHC and collagen type 1. (b, c, e and f) Treatment with either Dorsomorphin or sBMPR-1Af resulted in a significant decrease in the mean perimeter of centrally nucleated regenerating myofibres, compared with controls (100 regenerating fibres in the regenerating area of each animal were measured, and the mean size after exposure to Dorsomorphin or sBMPR-1Af expressed as the proportional change compared with the mean size of control regenerating myofibres). (b, d, e and g) Immunostaining for collagen type 1 was used to measure the degree of endomysial fibrosis, and a significant increase in the fibrotic index was observed in muscles exposed to either Dorsomorphin or sBMPR-1Af, compared with controls (the area of collagen type 1 expression in the regenerating area was measured in 1–3 sections for each animal, using ImageJ and changes with exposure to Dorsomorphin or sBMPR-1Af expressed as fold-difference compared with control). Six mice were used for each condition. Data are mean \pm S.E.M., where an asterisk denotes a significant difference from control ($P < 0.05$). Scale bars equal 100 μ m

Antagonism of BMP signalling by Noggin is employed during development to protect pre-myogenic cells, and expansion of the Noggin expression domain promotes ectopic myogenesis.^{11,12} We found that Noggin-mediated interference with BMP signalling was also redeployed during adult myogenesis. Noggin was upregulated as satellite cells differentiated, and knocking down Noggin resulted in more cells proliferating, while fewer differentiated. As Noggin is a secreted signalling molecule, it may also act in a paracrine manner to reduce BMP signalling in proliferating cells to potentiate and augment timely differentiation. Noggin expression in C2 cells is upregulated by exogenous BMP2,³⁶ and administration of Noggin to regenerating muscle reduces both pSmad1/5/8 and Id1 levels.³⁰ In addition, rhabdomyosarcoma cells express myogenic genes including MyoD and myogenin but form myotubes poorly, and have relatively high levels of *BMP4* and lower expression of *Noggin* than primary myoblasts.³⁷ Furthermore, specification of myogenic cells is unaffected in *Noggin*-null embryos, but differentiation is clearly perturbed, with meagre myotube formation during foetal myogenesis,³⁸ again suggesting a common role for

Noggin in supporting differentiation in both developmental and adult myogenesis.

We observed that inhibition of BMP signalling during muscle regeneration resulted in smaller regenerated myofibres. Similarly, *Id1*^{-/+} *Id3*^{-/-} mice also exhibit a muscle regeneration defect, with the cross-sectional area of regenerated myofibres being only ~50% of wild type.³⁰ These mice also had fewer proliferating satellite cells during regeneration.³⁰

In conclusion, BMP signalling is part of the programme that regulates routine satellite cell function. BMPs stimulate proliferation and prevent precocious differentiation to allow amplification of satellite cell-derived myoblasts. Noggin is then upregulated as satellite cell progeny differentiate, to antagonise BMP signalling and facilitate coordinated differentiation (Figure 9).

Materials and Methods

Isolation and culture of primary satellite cells and myoblasts. Adult (8–12 weeks old) C57BL10 mice were killed by cervical dislocation, and the EDL (or masseter for Figure 3b only) muscle isolated and

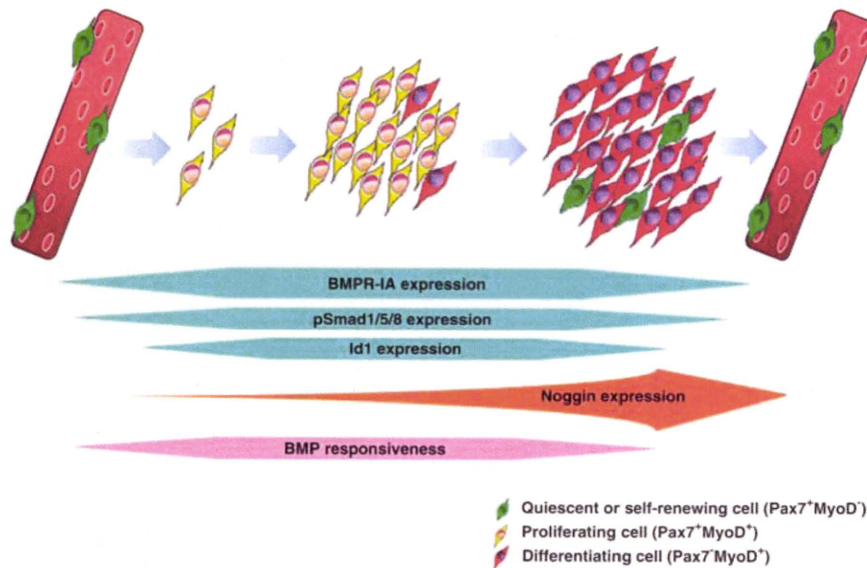


Figure 9 Role of BMP signalling during myogenic progression in satellite cells. During muscle repair and regeneration, quiescent Pax7⁺ satellite cells are activated to co-express Pax7 and MyoD. Satellite cell-derived myoblasts proliferate extensively before many cells then downregulate Pax7 and differentiate to either repair damaged muscle fibres or fuse together to generate new myofibres. Other satellite cells maintain Pax7 expression but lose MyoD, and self-renew to maintain a viable stem cell compartment. Normal BMP signalling through BMPR-1A and Smad1/5/8 phosphorylation is required during muscle repair/regeneration to allow the satellite cell-derived myoblast population to expand, by preventing precocious differentiation. BMP signalling operates through controlling Id levels, a negative regulator of MyoD and myogenic differentiation. As satellite cell progeny differentiate, Noggin is upregulated to antagonise the BMP signal, so facilitating the myogenic differentiation programme

digested in collagenase type1, as previously described.²⁵ Most satellite cells are mitotically quiescent in healthy adult muscle, so must first be activated and will then enter the cell cycle.² To induce satellite cell activation *in vitro*, myofibers and associated satellite cells were cultured in plating medium (DMEM supplemented with L-glutamine or GlutaMax (Sigma, Poole, Dorset, UK), 10% horse serum (PAA Laboratories, Yeovil, Somerset, UK), 0.5% chicken embryonic extract (MTX Lab Systems, Vienna, VA, USA) and 1% penicillin–streptomycin (Sigma)) at 37°C in 5% CO₂, as described previously.²⁴ To prepare plated satellite cells, either cells were removed from myofibers by enzymatic treatment with 0.125% trypsin–EDTA (Sigma) for 10 min at 37°C or allowed to migrate from isolated myofibres cultured on Matrigel. Satellite cells were then re-plated on Matrigel at equal density and maintained in proliferation medium (DMEM supplemented with L-glutamine or GlutaMAX, 20–30% foetal bovine serum, 1% chicken embryo extract, 10 ng/ml bFGF and 1% penicillin–streptomycin). Satellite cells were treated with 100 ng/ml recombinant BMP4 protein, (Peprotech, London, UK), 50 ng/ml recombinant Noggin protein (Peprotech), 200 ng/ml sBMPR-1Af (R&D systems, Abingdon, Oxfordshire, UK) or 0.1–3 μM Dorsomorphin (also known as Compound C; Calbiochem-MERCK-Beeston, Nottingham, UK) administered to the culture medium. In other experiments, satellite cells were switched from proliferation medium to differentiation medium (DMEM with L-glutamine or GlutaMax and supplemented with 2% horse serum and 1% penicillin–streptomycin) and cultured for 48 h with or without BMP4 (200 ng/ml). Myofibres and associated satellite cells or plated satellite cells were fixed with warm 4% paraformaldehyde (PFA).

antibodies were applied in PBS containing 0.1% Tween20 and incubated at 4°C overnight. HRP-conjugated secondary antibodies were used for visualisation by chemiluminescence (Fujifilm, Bedford, UK).

Immunostaining. Immunocytochemistry was as previously described.²⁵ Anti-BMPR-1A, anti-Ki67, anti-Smad5, anti-Smad4, anti-MyoD, anti-Noggin, anti-MyHC, anti-Pax7, anti-myogenin, anti-Id1 or anti-pSmad1/5/8 antibodies were applied at 4°C overnight. For co-immunostaining sections, frozen regenerating muscle cross-sections were fixed with 4% PFA, blocked using the M.O.M kit and incubated with either anti-pSmad1/5/8 and anti-MyoD antibodies or with anti-MyHC and anti-collagen type 1 antibodies. Immunostained myofibres, plated cells or cryosections were viewed on a Zeiss Axiophot 200M using Plan-Neofluar lenses (Zeiss, Welwyn Garden City, Hertfordshire, UK), or on a Nikon (Kingston upon Thames, Surrey, UK) C1si confocal using Plan-Fluor lenses. Digital images were acquired with a Zeiss AxioCam HRm Charge-Coupled Device using AxioVision software version 4.4. Images were optimised globally and assembled into figures using Adobe Photoshop. The Click-iT TUNEL Alexa fluor imaging assay (Invitrogen, Life Technologies, Paisley, UK) was used as per the manufacturer's instructions on satellite cells cultured for 24 h in proliferation medium containing either 1 μM or 5 μM Dorsomorphin (*n* = 3 mice).

CKM-luciferase reporter assay. Plated satellite cells were co-transfected with the *CKM firefly Luciferase* reporter plasmid (*CKM-LUCpCS2*) and *pcDNA3-Cre*-expressing control vector, *pcDNA3-mld1*-expressing vector²⁷ or *pcDEF3-caBMPR-1A*-expressing vector,⁷ using Lipofectamine LTX according to the manufacturer's instructions. The *Renilla* luciferase plasmid *pRL* (Promega Corporation, Madison, WI, USA), driven by a minimal tk promoter, was included as an internal control. Dorsomorphin was added to a final concentration of 5 μM. At 48 h post-transfection, the dual-Luciferase reporter assay (Promega) was performed according to the manufacturer's instructions and measured on an Anthos Lucy3 (JENCONS-PLS, East Grinstead, West Sussex, UK).

siRNA-mediated gene knockdown. The transfection of siRNA (Invitrogen Life Technologies) into primary satellite cell-derived myoblasts was performed using Lipofectamine 2000 reagent (Invitrogen Life Technologies) or Lipofectamine RNAiMAX (Invitrogen Life Technologies) as previously described.²⁵ Transfection of siRNA into single myofibers was carried out 12–16 h after isolation with Lipofectamine RNAiMAX (Invitrogen Life Technologies).²⁵ All samples were examined 1–3 days after the transfection. The following siRNA sequences were

Antibodies used in the study. Antibodies were obtained from the following sources. Rabbit anti-BMPR-1A (Alk-3) from Origen (San Diego, CA, USA) and a gift from Professor B. Kay;³⁹ rat anti-Ki67 from DakoCytomation (Ely, Cambridgeshire, UK); goat anti-Smad5, mouse anti-Smad4, mouse anti-MyoD and rabbit anti-MyoD antibodies were obtained from Santa Cruz (Santa Cruz, USA); goat anti-Noggin antibody was obtained from R&D systems; mouse anti-MyHC (MF20), anti-Pax7, anti-myogenin (F5D) and anti-β-tubulin antibodies (E7) were supplied by the DSHB (Iowa City, IA, USA); rabbit anti-pSmad1/5/8 antibody was from Cell Signalling Technology (Beverly, MA, USA); goat anti-collagen type 1 antibody was acquired from Southern Biotech (Birmingham, AL, USA). Mounting medium containing 4,6-diamidino-2-phenylindole (DAPI) to counterstain all nuclei and the M.O.M kit were both purchased from Vector Laboratories, Orton Southgate, Peterborough, UK.

Immunoblot analysis. Immunoblot analysis was performed as previously described.²⁵ Anti-BMPR-1A, anti-MyHC, anti-Pax7, anti-Myogenin or anti-β-tubulin

used: BMPR-1A siRNA: 5'-GAAGUGCUGGAUGAAAGCCUGAAUA-3', Smad4 siRNA: 5'-GGAGAGACGUUUAAGGUCCUCAA-3', Smad5 siRNA: 5'-CCUGGGAUUGUUGUCAAUUAU-3' and Noggin siRNA: 5'-CGACCCGGGCUUUAUGGCUCUUCG-3'. Control siRNAs were supplied by Invitrogen Life Technologies.

Muscle regeneration studies. Animal husbandry, breeding and experimental procedures were passed by the Ethical Review Process Committee of the King's College London, and were carried out in accordance with British law under the provisions of the Animals (Scientific Procedures) Act 1986. To assay pSmad1/5/8 expression, the gastrocnemius muscle of 10-week-old male C57BL/10 mice was injected with 50 μ l of 10 μ M cardiotoxin (Sigma) using a 29-G 1/2 insulin syringe. Muscles were removed 3 days later and immediately frozen in isopentane cooled in liquid nitrogen, and stored at -80°C before being cryosectioned and immunostained for pSmad1/5/8 and MyoD. To assay regenerative capacity in the presence of perturbed BMP signalling, the belly of both the left and right gastrocnemius muscles of 7- to 9-week-old male C57BL/10 mice were injected with 25 μ l of 10 μ M cardiotoxin (Sigma). At 1 and 3 days after cardiotoxin injection, 50 μ l of 10 μ M Dorsomorphin/DMSO dissolved in saline or 50 μ l of 100 μ g/ml sBMPR-1A dissolved in saline, were injected intramuscularly into the right gastrocnemius muscle at the same site as the cardiotoxin. Control solutions (same concentration of DMSO dissolved in saline for Dorsomorphin or BSA dissolved in saline for sBMPR-1A) were injected into the left muscle as a control. Muscles were removed 8 days after cardiotoxin injection and immediately frozen in isopentane cooled in liquid nitrogen and stored at -80°C . Transverse sections of muscle were cut with a cryostat and co-immunostained for MyHC and collagen type 1. Measurement of centrally nucleated regenerating myofibres and the area of endomysial fibrosis was performed using ImageJ software (developed by NIH and available for free download at <http://rsb.info.nih.gov/ij/>).

Statistical analysis. Data are presented as mean \pm standard deviation (S.D.) or mean \pm standard error (S.E.M.). Immunostained satellite cells from at least 10 myofibres were scored from each of at least three mice for each experiment. Significant differences between test conditions and controls were determined using Student *t*-test, wherein *P*-values < 0.05 were considered to be statistically significant.

Conflict of interest

The authors declare no conflict of interest.

Acknowledgements. We thank Dr. Stephen J. Tapscott for providing the *CKM-LUCpCS2* reporter plasmid; Dr. Robert Benezra for generously sharing *pcDNA3-mlf1* construct; Dr. Naohiro Hashimoto for helpful discussions and Paul Knopp for much help. We gratefully acknowledge colleagues who shared antibodies, including through the Developmental Studies Hybridoma Bank developed under the auspices of the NICHD and maintained by the University of Iowa. Y.O. was funded by the Muscular Dystrophy Campaign (RA3/737); F.C. is sponsored by the Association of International Cancer Research (07-0151); J.E.M. is backed by a Wellcome Trust university award. The laboratory of P.S.Z. is also supported by The Wellcome Trust, The Medical Research Council, the MYORES Network of Excellence (contract 511978) from the European Commission 6th Framework Programme and the collaborative Project OPTISTEM (Grant Agreement number: 223098) from the European Commission 7th Framework Programme.

1. Zammit PS. All muscle satellite cells are equal, but are some more equal than others? *J Cell Sci* 2008; **121**: 2975–2982.
2. Zammit PS, Golding JP, Nagata Y, Hudon V, Partridge TA, Beauchamp JR. Muscle satellite cells adopt divergent fates: a mechanism for self-renewal? *J Cell Biol* 2004; **166**: 347–357.
3. Halevy O, Piestun Y, Alouh MZ, Rosser BW, Rinkevich Y, Reshef R *et al*. Pattern of Pax7 expression during myogenesis in the posthatch chicken establishes a model for satellite cell differentiation and renewal. *Dev Dyn* 2004; **231**: 489–502.
4. Collins CA, Olsen I, Zammit PS, Heslop L, Petrie A, Partridge TA *et al*. Stem cell function, self-renewal, and behavioral heterogeneity of cells from the adult muscle satellite cell niche. *Cell* 2005; **122**: 289–301.
5. Feng XH, Derynck R. Specificity and versatility in TGF-beta signaling through Smads. *Annu Rev Cell Dev Biol* 2005; **21**: 659–693.

6. Hollnagel A, Oehlmann V, Heymer J, Ruther U, Nordheim A. Id genes are direct targets of bone morphogenetic protein induction in embryonic stem cells. *J Biol Chem* 1999; **274**: 19838–19845.
7. Katagiri T, Imada M, Yanai T, Suda T, Takahashi N, Kamijo R. Identification of a BMP-responsive element in Id1, the gene for inhibition of myogenesis. *Genes Cells* 2002; **7**: 949–960.
8. Korchynskiy O, ten Dijke P. Identification and functional characterization of distinct critically important bone morphogenetic protein-specific response elements in the Id1 promoter. *J Biol Chem* 2002; **277**: 4883–4891.
9. Jen Y, Weintraub H, Benezra R. Overexpression of Id protein inhibits the muscle differentiation program: *in vivo* association of Id with E2A proteins. *Genes Dev* 1992; **6**: 1466–1479.
10. Wozney JM, Rosen V, Celeste AJ, Mitscock LM, Whitters MJ, Kriz RW *et al*. Novel regulators of bone formation: molecular clones and activities. *Science* 1988; **242**: 1528–1534.
11. Reshef R, Maroto M, Lassar AB. Regulation of dorsal somitic cell fates: BMPs and Noggin control the timing and pattern of myogenic regulator expression. *Genes Dev* 1998; **12**: 290–303.
12. Réem-Kalma Y, Lamb T, Frank D. Competition between noggin and bone morphogenetic protein 4 activities may regulate dorsalization during *Xenopus* development. *Proc Natl Acad Sci USA* 1995; **92**: 12141–12145.
13. Hirsinger E, Duprez D, Jouve C, Malapert P, Cooke J, Pourquie O. Noggin acts downstream of Wnt and Sonic Hedgehog to antagonize BMP4 in avian somite patterning. *Development* 1997; **124**: 4605–4614.
14. Amthor H, Christ B, Weil M, Patel K. The importance of timing differentiation during limb muscle development. *Curr Biol* 1998; **8**: 642–652.
15. Wada MR, Inagawa-Ogashiwa M, Shimizu S, Yasumoto S, Hashimoto N. Generation of different fates from multipotent muscle stem cells. *Development* 2002; **129**: 2987–2995.
16. Katagiri T, Yamaguchi A, Komaki M, Abe E, Takahashi N, Ikeda T *et al*. Bone morphogenetic protein-2 converts the differentiation pathway of C2C12 myoblasts into the osteoblast lineage. *J Cell Biol* 1994; **127**: 1755–1766.
17. Asakura A, Komaki M, Rudnicki M. Muscle satellite cells are multipotential stem cells that exhibit myogenic, osteogenic, and adipogenic differentiation. *Differentiation* 2001; **68**: 245–253.
18. Dahlqvist C, Blokzijl A, Chapman G, Falk A, Dannaeus K, Ibanez CF *et al*. Functional Notch signaling is required for BMP4-induced inhibition of myogenic differentiation. *Development* 2003; **130**: 6089–6099.
19. Kaplan FS, Shen Q, Lounev V, Seemann P, Groppe J, Katagiri T *et al*. Skeletal metamorphosis in fibrodysplasia ossificans progressiva (FOP). *J Bone Miner Metab* 2008; **26**: 521–530.
20. Lounev VY, Ramachandran R, Wosczyzna MN, Yamamoto M, Maidment AD, Shore EM *et al*. Identification of progenitor cells that contribute to heterotopic skeletogenesis. *J Bone Joint Surg Am* 2009; **91**: 652–663.
21. Yu PB, Deng DY, Lai CS, Hong CC, Cuny GD, Bouxsein ML *et al*. BMP type I receptor inhibition reduces heterotopic ossification. *Nat Med* 2008; **14**: 1363–1369.
22. Namiki M, Akiyama S, Katagiri T, Suzuki A, Ueno N, Yamaji N *et al*. A kinase domain-truncated type I receptor blocks bone morphogenetic protein-2-induced signal transduction in C2C12 myoblasts. *J Biol Chem* 1997; **272**: 22046–22052.
23. Kodaira K, Imada M, Goto M, Tomoyasu A, Fukuda T, Kamijo R *et al*. Purification and identification of a BMP-like factor from bovine serum. *Biochem Biophys Res Commun* 2006; **345**: 1224–1231.
24. Ono Y, Boldrin L, Knopp P, Morgan JE, Zammit PS. Muscle satellite cells are a functionally heterogeneous population in both somite-derived and branchiomeric muscles. *Dev Biol* 2010; **337**: 29–41.
25. Ono Y, Gnocchi VF, Zammit PS, Nagatomi R. Presenilin-1 acts via Id1 to regulate the function of muscle satellite cells in a gamma-secretase-independent manner. *J Cell Sci* 2009; **122**: 4427–4438.
26. Yu PB, Hong CC, Sachidanandan C, Babbitt JL, Deng DY, Hoyng SA *et al*. Dorsomorphin inhibits BMP signals required for embryogenesis and iron metabolism. *Nat Chem Biol* 2008; **4**: 33–41.
27. Benezra R, Davis RL, Lockshon D, Turner DL, Weintraub H. The protein Id: a negative regulator of helix-loop-helix DNA binding proteins. *Cell* 1990; **61**: 49–59.
28. Akiyama S, Katagiri T, Namiki M, Yamaji N, Yamamoto N, Miyama K *et al*. Constitutively active BMP type I receptors transduce BMP-2 signals without the ligand in C2C12 myoblasts. *Exp Cell Res* 1997; **235**: 362–369.
29. Kumar D, Shadrach JL, Wagers AJ, Lassar AB. Id3 is a direct transcriptional target of Pax7 in quiescent satellite cells. *Mol Biol Cell* 2009; **20**: 3170–3177.
30. Clever JL, Sakai Y, Wang RA, Schneider R. Inefficient skeletal muscle repair in inhibitor of differentiation (Id) knockout mice suggests a crucial role for bmp signaling during adult muscle regeneration. *Am J Physiol Cell Physiol* 2010; **298**: C1087–C1099.
31. Sterrenburg E, van der Wees CG, White SJ, Turk R, de Menezes RX, van Ommen GJ *et al*. Gene expression profiling highlights defective myogenesis in DMD patients and a possible role for bone morphogenetic protein 4. *Neurobiol Dis* 2006; **23**: 228–236.

32. Xiao Q, Du Y, Wu W, Yip HK. Bone morphogenetic proteins mediate cellular response and, together with Noggin, regulate astrocyte differentiation after spinal cord injury. *Exp Neurol* 2010; **221**: 353–366.
33. Liu R, Ginn SL, Lek M, North KN, Alexander IE, Little DG *et al*. Myoblast sensitivity and fibroblast insensitivity to osteogenic conversion by BMP-2 correlates with the expression of *Bmpr-1a*. *BMC Musculoskelet Disord* 2009; **10**: 51.
34. Conboy IM, Rando TA. The regulation of Notch signaling controls satellite cell activation and cell fate determination in postnatal myogenesis. *Dev Cell* 2002; **3**: 397–409.
35. Nakashima A, Katagiri T, Tamura M. Cross-talk between Wnt and bone morphogenetic protein 2 (BMP-2) signaling in differentiation pathway of C2C12 myoblasts. *J Biol Chem* 2005; **280**: 37660–37668.
36. Takayama K, Suzuki A, Manaka T, Taguchi S, Hashimoto Y, Imai Y *et al*. RNA interference for noggin enhances the biological activity of bone morphogenetic proteins *in vivo* and *in vitro*. *J Bone Miner Metab* 2009; **27**: 402–411.
37. Goldstein M, Meller I, Orr-Urtreger A. FGFR1 over-expression in primary rhabdomyosarcoma tumors is associated with hypomethylation of a 5' CpG island and abnormal expression of the AKT1, NOG, and BMP4 genes. *Genes Chromosomes Cancer* 2007; **46**: 1028–1038.
38. Tytkanowski P, Mebis L, Luyten FP. The Noggin null mouse phenotype is strain dependent and haploinsufficiency leads to skeletal defects. *Dev Dyn* 2006; **235**: 1599–1607.
39. Kariyawasam HH, Xanthou G, Barkans J, Aizen M, Kay AB, Robinson DS. Basal expression of bone morphogenetic protein receptor is reduced in mild asthma. *Am J Respir Crit Care Med* 2008; **177**: 1074–1081.